National Institute of Environmental Health Sciences

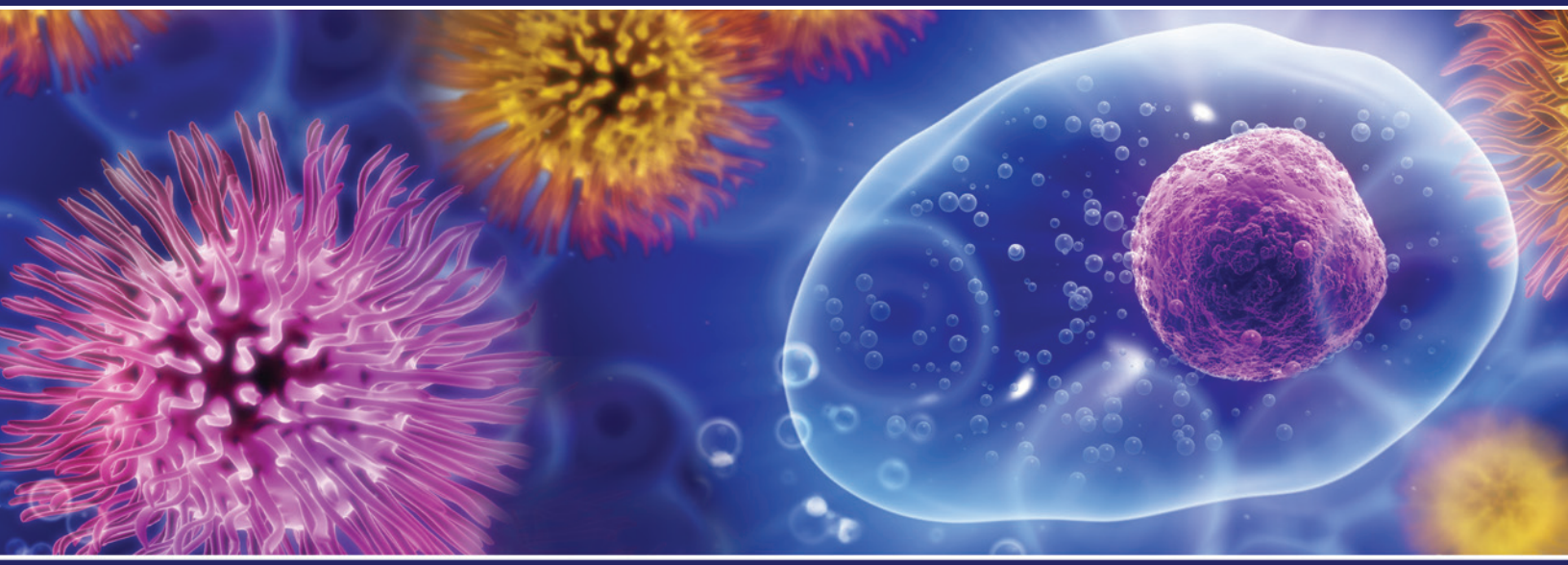

19TH ANNUAL

NIEHS Science Day

November 19, 2021

National Institutes of Health • U.S. Department of Health and Human Services

DEPARTMENT OF HEALTH & HUMAN SERVICES Public Health Service

Hans Luecke, Ph.D.
Associate Scientific Director
Tel: 301-335-1915
hans.luecke@nih.gov

National Institutes of Health
National Institute of
Environmental Health Sciences
Division of Intramural Research
Bldg. 101, Room A2
P. O. Box 12233, Mail Drop A2-09
Research Triangle Park, NC 27709

November 19, 2021

Dear NIEHS scientists and guests:

On behalf of Dr. Rick Woychik, Director of NIEHS and NTP, I would like to welcome you to Science Day. This event is a celebration of our research achievements, and is a way to recognize and honor some of our outstanding scientists. This year we are holding Science Day as a virtual event due to the ongoing COVID-19 pandemic.

I especially wish to thank the outstanding members of the NIEHS IT community for their help in transforming Science Day into a virtual event that hopefully maintains many aspects of past in-person Science Day events.

We have invited environmental health scientists from across North Carolina to join us today and participate as judges. We appreciate their efforts and welcome them to the to our virtual NIEHS world. Hopefully we will be able to see you on campus in the near future.

We are also grateful to the DIR and DNTP Scientists who are serving as judges for the poster presentation competition.

Finally, I would also like to acknowledge the other members of the NIEHS Science Day Steering Committee, Drs. Abee Boyles, Heather Henry, Anton Jetten, Kaitlyn Lawrence, Leping Li, Negin Martin, Alex Merrick, Arun Pandiri, Amanda Riccio, Thad Schug, Erik Tokar, Jack Taylor, and Karina Rodriguez. Without their efforts Science Day would be possible.

Please enjoy the Science Day events and join me in celebrating some of our scientific achievements.

Sincerely,

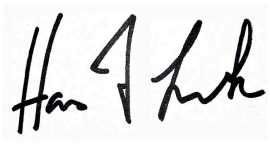

Hans Luecke, Ph.D.

Extramural Judges

Ramji Bhandari University of North Carolina at Greensboro	Megen Culpepper Appalachian State University
Keith Erickson University of North Carolina at Greensboro	Mary Foster Duke University
Rebecca Fry University of North Carolina	Kymberly Gowdy Ohio State College of Medicine
Jack D. Griffith University of North Carolina	Carol Hamilton Research Triangle Institute
Samir Kelada University of North Carolina	Edward Levin Duke University
Shuang Lim North Carolina State University	Kun Lu University of North Carolina
Alex Marshall North Carolina Central University	Heather Patisaul North Carolina State University
David Reif North Carolina State University	Robert Tighe Duke University
Xiaohe Yang North Carolina Central University	Mark Zylka University of North Carolina

Intramural Judges

Donna Baird	Guang Hu	Roel Schaaper
Terry Blankenship-Paris	Chandra Jackson	Robin Stanley
John Cidlowski	Anton Jetten	Erik Tokar
Franco DeMayo	Anne Marie Jukic	Paul Wade
Darlene Dixon	Xiaoling Li	Clare Weinberg
Paul Doetsch	Marcos Morgan	Carmen Williams
Serena Dudek	Geoff Muellller	Scott Williams
Kelly Ferguson	Barbara Nicol	Jerry Yakel
Kevin Gerrish	Lars Pedersen	Humphrey Yao
Dmitry Gordenin	Kristen Ryan	Shanshan Zhao
	Dale Sandler	

NIEHS Science Day

November 19, 2021

ZoomGov meeting
bit.ly/NIEHS_Science_Day

Opening Remarks:

9:00-9:15 am	Introduction and Welcoming Remarks Rick Woychik, Ph.D., NIEHS Director Hans Luecke, Ph.D., Chair, Science Day Committee

Oral Presentations Session 1:

9:15-10:30 am	5 Oral Presentations by Fellows/Students/Technicians
9:15-9:30 am	#1. Liu Y, Grimm SA, Williams JG, Deterding LJ, Lih FB, and Wade PA. **Reprogramming the Circadian Metabolism by Methionine Restriction** (ESCBL, DIR)
9:30-9:45 am	#2. Radzicki D, McCann KE, Alexander GM, and Dudek SM. **Hippocampal Area CA2 Activity Supports Resilience Following an Acute Social Stress**. (NL, DIR)
9:45-10:00 am	#3. Tong X, Akhtari F, House J, Burkholder A, Schmitt C, Fargo D, Hall JE, Vsevolozhskaya O, Zaykin D, and Motsinger-Reif A. **Cataloging gene-environment interaction candidate SNPs for over 3,000 UK Biobank disease phenotypes through variance loci analysis**. (BCBB, DIR)
10:00-10:15 am	#4. Niehoff NM, Terry M, Bookwalter DB, Kaufman JD, O'Brien KM, Sandler DP, and White AJ. **Air pollution and breast cancer: an examination of modification by underlying familial breast cancer risk**. (EB, DIR)
10:15-10:30 am	#5. Hayne CK, Stewart ZD, Butay KJ, Borgnia MJ, and Stanley RE. **Novel insights into the structure, function, and regulation of human tRNA splicing**. (STL, DIR)
10:30-10:45 am	Break

Morning Poster Session:

10:45 am-12:00 pm Presentation of Posters 1-30

Time	Room 1 Posters 1-5	Room 2 Poster 6-10	Room 3 Posters 11-15	Room 4 Posters 16-20	Room 5 Posters 21-25	Room 6 Posters 26-30
10:45am - 11:00am	Al-Hasan, DM	Bermek, O	Collier, JB	Dickson, MJ	Gaston, SA	Headley, KM
11:00am - 11:15am	Alagna, NS	Bommarito, PA	Davalos, AD	Fan, W	Goldberg, M	Hudson, K
11:15am - 11:30am	Alexander, GM	Bridges, KA	Dee, RA	Foo, AC	Gordon, J	Jaguva Vasudevan, A
11:30am - 11:45am	Amato III, CM	Chen, I	Degtyareva, N	Frazier, MN	Goulding, DR	Kar, A
11:45am - 12:00pm	Arana, M	Chi, RA	Diaz Jimenez, DO	Garcia Villada, L	Gullett, LR	Kocaman, S

12:00 pm-1:00 pm Break

Afternoon Poster Session:

1:00 pm-2:15 pm Presentation of Posters 31-55

Time	Room 7 Posters 31-35	Room 8 Posters 36-40	Room 9 Posters 41-45	Room 10 Posters 46-49	Room 11 Posters 50-55
1:00pm - 1:15pm	Kockler, ZW	Pradhan, T	Silver II, BB	Von Holle, AF	Xu, Q
1:15pm - 1:30pm	Langton, CR	Rattan, S	Srivastava, C	Weick, MI	Yan, Y
1:30pm - 1:45pm	Li, R	Riley, NM	Stevens, DR	Wilson, IM	Yi, M
1:45pm - 2:00pm	Li, W-N	Salven, DS	Subramanian, A	Woo, JM	Yu, H
2:00pm - 2:15pm	Min, J	Savy, V	Tumbale, PP		Morgan, M

2:15 pm-2:30 pm Break

Oral Presentations Session 2:

2:30 pm-3:45 pm 5 Oral Presentations by Fellows/Students/Technicians

2:30-2:45 pm #6. Sakamachi Y, Solis A, Johnson CG, Meng X, Hussain S, O'Dwyer DN, Mehta S, Trempus CS, Thomas SY, Li J, Zhou L, Karmaus PW, McGrath JA, Lipinski JH, Gibson K, Kass DJ, Gleiberman A, Walts A, Invernizzi R, Molyneaux PL, Yang IV, Zhang Y, Kaminski N, Schwartz DA, Gudkov AV, and Garantziotis S. **Toll-Like-Receptor 5 Protects Against Pulmonary Fibrosis by Reducing Lung Dysbiosis**. (IIDL, DIR)

2:45-3:00 pm	#7. Baptissart M, Papas B, Puviindran B, Li Y, and Morgan M. **Poly(A) tail dynamics during cell differentiation show transcript compartmentalization and specific post-transcriptional regulation**. (RDBL, DIR)
3:00-3:15 pm	#8. Calvert ME, Kalra B, Patel A, Kumar A, and Shaw ND. **Serum and urine profiles of TGF-β superfamily members in reproductive age women**. (CRB, DIR)
3:15-3:30 pm	#9. Wu X, Dixon D, and Tokar EJ. **Engineering Human Neural Organoids to Explore Developmental Neurotoxicity Induced by Chronic Arsenic Exposure**. (MTB, DNTP)
3:30-3:45 pm	#10. Zhou Z, Lujan SA, Burkholder AB, St. Charles J, Dahl J, Farrell CE, Williams JS, and Kunkel TA. **How asymmetric DNA replication achieves high and symmetrical fidelity**. (GISBL, DIR)
3:45-4:00 pm	Break
4:00-5:00 pm	Science Day Award Ceremony and Closing Remarks

Poster Presentations

Poster 1. Al-Hasan DM, Gaston SA, Jackson II B, and Jackson CL.
Neighborhood social cohesion and obesity across racial/ethnic groups in the United States(EB).

Poster 2. Alagna NS, and Schaaper RM.
Control of dNTP Pools and Their Role in Genome Integrity(GISBL).

Poster 3. Alexander GM, Carstens KE, Gloss B, Lilly SR, Slay BS, Martin NP, and Dudek SM.
Potential role of serotype and perineuronal nets in the preferential expression of adeno-associated virus-packaged genetic cargo in hippocampal CA2 neurons(NL).

Poster 4. Amato CM, and Yao HH.
A hindlimb derived cell population is necessary in penis formation(RDBL).

Poster 5. Arana ME, Williams JS, Tumbale PP, Rana J, Williams SR, and Kunkel TA.
DNA Ligase 1: Ligation, Fidelity and a Role In Maintaining Genome Stability(GISBL).

Poster 6. Bermek O, and Williams SR.
Structure-Function Analysis of the Herpes Simplex Virus-1 Primosome(GISBL).

Poster 7. Bommarito PA, Cantonwine DE, McElrath TF, and Ferguson KK.
Characterizing fetal growth trajectories among small-for-gestational age births in the LIFECODES Birth Cohort(EB).

Poster 8. Bridges KA, Nicol B, and Yao H.
The Potential Role of Runx1 in Ovarian Cancer and Pathologies(RDBL).

Poster 9. Chen I, Birla S, and Tokar E.
A human pluripotent stem cell-based high-throughput platform with artificial intelligence technology to screen for developmental toxicants(MTB).

Poster 10. Chi RA, Xu X, Li J, Kirsanov O, Geyer C, Xu X, Willson C, Hu G, Huang C, and DeMayo F.
WNK1 is vital for male fertility through regulating both meiotic initiation and progression during spermatogenesis(RDBL).

Poster 11. Collier JB, Roh Y, Srivastava C, Kang H, Grimm S, and Jetten AM.
GLIS3-Deficiency in the Maturing Kidney Leads to Metabolic Reprogramming and Polycystic Kidneys(IIDL).

Poster 12. Davalos AD, Ferguson KK, and Zhao S.
IDENTIFYING MULTIVARIATE LATENT CLASS GROWTH TRAJECTORIES VIA THE BAYESIAN TENSOR MIXTURE OF REGRESSIONS MODEL(BCBB).

Poster 13. Dee RA, Blystone CR, Cora MC, Shockley KR, Stout MD, and Waidyanatha S.
A 14-day toxicity class comparison study of nine phenolic benzotriazoles in male Sprague Dawley rats(STB).

Poster 14. Degtyareva NP, Placentra VC, Klimczak LJ, Gabel SA, Mueller GA, Smirnova TI, and Doetsch PW.
Exposure to an environmentally relevant oxidizer, potassium bromate, produces novel metabolic and mutational signatures that are distinct from the signatures of other redox stress agents(GISBL).

Poster 15. Diaz-Jimenez DO, and Cidlowski JA.
Glucocorticoids suppress NLRP3 Inflammasome activation through transcriptional metabolic reprogramming of the IRG-1 in macrophages(STL).

Poster 16. Dickson MJ, Ray M, and DeMayo FJ.
Utilization of Soluble Cre for Gene Editing in Mouse Endometrial Epithelial Organoids.(RDBL).

Poster 17. Fan W, and Xiaoling L.
Lipid Metabolism in Neural Differentiation of Embryonic Stem Cells (STL).

Poster 18. Foo AC, Chen S, Martin N, and Mueller GA.
The Mosquito Protein AEG12 as a Scaffold for Novel Antiviral Therapeutics(GISBL).

Poster 19. Frazier MN, Dillard LB, Krahn JM, Perera L, Williams JG, Wilson IM, Stewart Z, Pillon MC, Deterding LJ, Borgnia MJ, and Stanley RE.
Searching for U: Cryo-EM Structures of the SARS-CoV-2 Endoribonuclease Nsp15 Reveal Insight into Nuclease Specificity and Dynamics(STL).

Poster 20. Garcia Villada L, Brooks AM, Degtyareva NP, and Doetsch PW.
Mutations in the essential gene spoT confer resistance to ciprofloxacin in the microbial pathogen Pseudomonas aeruginosa(GISBL).

Poster 21. Gaston Harrison SA, Lawrence KG, Sandler DP, and Jackson CL.
Neighborhood Deprivation and Sleep Health in a Racially/Ethnic Diverse Cohort of U.S. Women (EB).

Poster 22. Goldberg M, D'Aloisio AA, O'Brien KM, Zhao S, and Sandler DP.
Early-life exposures and age at breast development: Implications for breast cancer risk(EB).

Poster 23. Gordon J, Viverette E, Borgnia MJ, and Stanley RE.
Structure of the multi-functional human scaffolding protein PELP1 bound to WDR18 reveals insight into its diverse cellular functions. (STL).

Poster 24. Goulding DR, Wiltshire RA, Shi M, and Blankenship-Paris TL.
Identification of refinements in a murine model of lipopolysaccharide systemic inflammation in C57BL/6 mice(CMB).

Poster 25. Gullett LR, Alhasan DM, Jackson II B, Gaston SA, Kawachi I, and Jackson CL.
Neighborhood Social Cohesion and Serious Psychological Distress among Asian, Black, Hispanic/Latinx, and White Men and Women in the United States(EB).

Poster 26. Headley KM, Chrysovergis K, and Wade P.
Characterization of reproductive and hormonal defects in mutant NuRD complex members, CHD4 and MTA3, in mouse model systems.(ESCBL).

Poster 27. Hudson K, Klimczak LJ, Sterling JF, Burkholder AB, Saini N, Mieczkowski P, and Gordenin DA.
Signature motif of glycidamide-induced hypermutation in single-stranded DNA is ubiquitous in human cancers(GISBL).

Poster 28. Jaguva Vasudevan A, Riccio A, Appel C, and R. Scott W.
ZATT (ZNF451) is a novel nuclear RNA/DNA hybrid cleaving enzyme (GISBL).

Poster 29. Kar A, Degtyareva N, and Doetsch PW.
Dysregulation of NTHL1 causes sensitivity to cisplatin in human cells (GISBL).

Poster 30. Kocaman S, Kocaman S, Lo Y, Krahn JM, Sobhany M, Dandey VP, Petrovich M, Williams JG, Deterding LJ, Borgnia MJ, and Stanley RR.
Communication network within Rix7 AAA-ATPase to drive ribosome assembly(STL).

Poster 31. Kockler ZW, Klimczak LJ, Bostan H, Li J, Roberts SA, and Gordenin DA.
RNA editing by APOBEC3 cytidine deaminases(GISBL).

Poster 32. Langton CR, Harmon QE, Upson K, and Baird DD.
Soy-based infant formula feeding and uterine fibroid incidence in a prospective ultrasound study of African American women(EB).

Poster 33. Li R, Wang T, Wu S, and DeMayo F.
TRIM28 regulates uterine function by modulating steroid receptor signaling(RDBL).

Poster 34. Li W, Emery O, Wang T, Zhou L, Wu S, and DeMayo F.
The Role of Serum Response Factor in Regulating Hormonal Responsiveness in the Uterine Function(RDBL).

Poster 35. Min J, Pomés A, Patil S, Pedersen LC, and Mueller GA.
Ternary crystal structure of neutralizing antibodies complexed with major peanut allergen Ara h 2(GISBL).

Poster 36. Pradhan T, Pradhan T, Kang H, Grimm S, and Jetten AM.
GLIS3: A critical player in pancreatic ductal cell function (IIDL).

Poster 37. Rattan S, Liu C, Rodriguez K, and Yao HH.
Two Paths Diverged in the Fetal Mouse Ovary, Sorry I Could Not Travel Both(RDBL).

Poster 38. Riley NM, Alhasan DM, Jackson II W, and Jackson CL.
Food Insecurity and Sleep Health by Race/Ethnicity in the United States(EB).

Poster 39. Salven DS, Parsons R, Tumbale P, and Williams R.
Characterization of Treacle DNA Binding and Disease Mutations in Treacher Collins Syndrome(GISBL).

Poster 40. Savy V, Shi M, Stein P, and Williams CJ.
PMCA1 regulates calcium signals at fertilization(RDBL).

Poster 41. Silver BB, Gerrish K, and Tokar E.
Cell-free DNA is predictive of cellular differentiation status in cardiac organoids (MTB).

Poster 42. Srivastava C, Srivastava C, Grimm S, Randall T, DeGraff LM, Gruzdev A, and Jetten AM.
Loss of JAZF1 protects against High-Fat Diet-Induced gut microbial dysbiosis and Nonalcoholic Fatty Liver Disease(IIDL).

Poster 43. Stevens DR, Keil AP, Bommarito P, McElrath T, Trasande L, Barrett ES, Bush NR, Nguyen R, Sathyanarayana S, Swan S, and Ferguson KK.
Urinary phthalate metabolite mixtures in pregnancy in relation to fetal growth(EB).

Poster 44. Subramanian A, Steiner AZ, Weinberg CR, and Jukic AZ.
Preconception Vitamin D and Miscarriage in a Prospective Time to Pregnancy Study(EB).

Poster 45. Tumbale PP, Jurkiw T, Schellenberg MJ, Riccio A, Cunningham-Rundles C, O'Brien P, and Williams R.
High-Resolution X-Ray Structures of DNA ligase 1 Reveal the Molecular Mechanisms of High-Fidelity DNA Ligation and LIG1 Syndrome(GISBL).

Poster 46. Von Holle AF, O'Brien KM, Sandler DP, Janicek R, Karagas MR, White AJ, Jackson BP, and Weinberg CR.
Toenail and serum measures as biomarkers of iron levels(BCBB).

Poster 47. Weick MI, Chen I, Silver B, Gladwell W, Wu X, Tokar E, Foley JF, Merrick BA, and Gerrish K.
Exploration of Cell-Free DNA as a Potential Biomarker of Teratogenicity Using a Human Embryonic Stem Cell Culture Model (STL).

Poster 48. Wilson IM, Frazier MN, Li J, Randall T, and Stanley RE.
Functional characterization of the SARS-CoV-2 Nsp15 endoribonuclease N-terminal domain and beyond.(STL).

Poster 49. Woo JM, Bookwalter DB, and Sandler DP.
Socioeconomic Position During Childhood and Over the Life Course and its Association with Obesity in Adulthood(EB).

Poster 51. Xu Q, and Li X.
Liver cancer cells that survive methionine restriction develop phenotypes of persistent cancer cells(STL).

Poster 52. Yan Y, Shi M, Fannin R, Yu L, Liu J, Castro L, and Dixon D.
Cadmium exposure alters migration dynamics and increases heterogeneity of human uterine fibroid cells - insights from time-lapse analysis(MTB).

Poster 53. Yi M, Jukic AZ, and DeMayo FJ.
Impact of Vitamin D Deficiency on Defective In Vivo and In Vitro Decidualization(RDBL).

Poster 54. Yu H, Wang J, Lackford B, Bennett B, Li J, and Hu G.
INO80 Remodels Bivalent Chromatin in Pluripotent State Transition(ESCBL).

Poster 55. Morgan M, Kumar L, Li Y, Baptissart M, and Gupta A.
Role of TUT4 and TUT7 in spermatogonia differentiation(RDBL).

Oral Presentation 1

Reprogramming the Circadian Metabolism by Methionine Restriction

Liu Y, Grimm SA, Williams JG, Deterding LJ, Lih FB, and Wade PA
Eukaryotic Transcriptional Regulation, Integrative Bioinformatics Support Group, Mass Spectrometry Research and Support Group, ESCBL, DIR, NIEHS

Accumulating evidence reveals that the circadian clock is integral to maintenance of metabolic homeostasis and that diet can dramatically remodel circadian metabolism. Recent studies show that dietary methionine restriction (MR) improves metabolic health and extends lifespan. However, the effects of MR on the circadian clock and the underlying mechanisms have been unclear.

In this study, C57BL/6 J mice were submitted to control amino acid diet (8.2% methionine, w/w) or methionine deprivation diet (MD, No methionine) for 3 weeks. We demonstrate that serum methionine was dramatically deceased by MD. Interestingly, both serum methionine and S-adenosylmethionine (SAM) exhibited an oscillating pattern in the mice fed on MD, but not in control animals. We found MD led to a reduction in body weight and serum cholesterol level. Moreover, MD increased energy expenditure specifically during the dark phase.

We performed RNA-seq using liver tissue collected at six time points to explore the effects of MD on the circadian gene expression. Our transcriptomic analysis showed that 1,403 genes lost rhythmicity upon the MD whereas there were 3,287 genes oscillating de novo under MD in liver. The number of cyclic genes under both nutritional conditions were 2,869. The expression of hepatic fibroblast growth factor 21 (FGF21), which is a critical mediator of the physiological effects of dietary MR, was specifically induced by MD during dark phase. Meanwhile, the rhythmicity of lipogenic genes, including *Srebp1*, *Elovl3* and *Elovl5*, was compromised by MD.

Methionine metabolism plays a pivotal role in the process of methylation. To explore the effects of MD on RNA methylation, we performed the methylated RNA immunoprecipitation sequencing (MeRIP-seq) for liver collected at ZT9 and ZT21 with antibody against N6-methyladenosine (m6A). We found that m6A was predominantly enriched in 3'UTRs and CDS under both control and MD diets. The m6A in the 3' UTR of SAM Synthesis MAT2A was reduced by MD. Notably, activating transcription factor (ATF)3, which displaying rhythmicity only under MD, exhibited a higher expression level accompanying with the reduced m6A modification at ZT21 under MD.

We also found that MD reduced the tri-methylation of histone marks, including H3K4me3, H3K9me3 and H3K36me3. We profiled genomic H3K36me3 and H3K9me3 by Cleavage Under Targets & Tagmentation (CUT&TAG) in liver tissue collected at ZT9 and ZT21. The H3K36me3 and H3K4me3 peaks on lipogenic genes were reduced by MD at ZT21. These results suggest that dietary methionine restriction improves the metabolic health by reprogramming of circadian metabolism, which is mediated by modulating the methylation of histone and RNA.

Oral Presentation 2

Hippocampal Area CA2 Activity Supports Resilience Following an Acute Social Stress

Radzicki D, McCann KE, Alexander GM, and Dudek SM
Synaptic and Developmental Plasticity, NL, DIR, NIEHS

Neuronal activity in the hippocampus is critical for memory acquisition and retrieval and influences an animal's response to stress. Moreover, the molecularly distinct principal neurons of hippocampal area CA2 are required for social recognition memory and aggression in rodents. Given the high concentration of the mineralocorticoid stress hormone receptor in area CA2, this region is also positioned to play an important role in the greater hippocampal stress response. To further interrogate the effects of stress on CA2 dependent behaviors, we chemogenetically manipulated neuronal activity *in vivo* during an acute, socially derived stressor and tested whether memory for the defeat was influenced.

We used the acute social defeat (ASD) paradigm wherein male subject C57 mice undergo a five-minute bout of social defeat in the home cage of a large male CD1 aggressor. 24 hours after the defeat, we observed that defeated mice spent, on average, significantly less time investigating a novel CD1 mouse when compared to control mice that had not been exposed to the aggressor mice (50.3 +/-10.5 vs. 99.4 +/-5.1 s, n=22,18, p=0.0001). Furthermore, we found that this avoidant phenotype persisted for up to one month following a single defeat: mice exhibited either a susceptible/avoidant or a resilient/investigative behavioral phenotype when CA2 activity was left unperturbed. When CA2 activity was inhibited using cell-type specific expression of the inhibitory Gi-DREADD receptor during the defeat, however, subject mice exhibited a significantly higher amount of social avoidance one day later when compared to defeated littermates not expressing the DREADDs (241.6 +/-12.7 vs. 188.6 +/-16.4 s, n=18,18, p=0.02). This increased avoidance was driven by a loss of the 'resilient' population of defeated mice. We also observed ASD-dependent changes in neuronal activity following social investigation, as measured by the immediate early gene (IEG) c*fos*, in both hippocampal and extrahippocampal brain regions. Given CA2's known role in aggression, we asked whether inhibition of CA2 also modulated the behavior of subjects during the defeat itself. We observed a significant reduction in the amount of defensive submission during defeat when CA2 was inhibited (24.5 +/-5.1 vs. 44.1 +/-6.3 s, n=18,18, p=0.02). Interestingly, when CA2 activity was left unperturbed during defeat and inhibited immediately after, we observed no significant difference in social investigation at 24 hours when comparing defeated animals with the Gi-DREADD expressed or without (176.0 +/-16.6 vs. 186.2 +/-18.9 , n=10,13).

Taken together these results indicate that acute social defeat is a robust social stress paradigm that can persist for weeks in a more susceptible population of mice. Furthermore, inhibition of CA2 can not only alter an animal's defensive behavior when subjected to threat or aggression but leads to a more socially avoidant phenotype following acute social defeat.

Oral Presentation 3

Cataloging gene-environment interaction candidate SNPs for over 3,000 UK Biobank disease phenotypes through variance loci analysis

Tong X, Akhtari F, House J, Burkholder A, Schmitt C, Fargo D, Hall JE, Vsevolozhskaya O, Zaykin D, and Motsinger-Reif A

Biostatistics and Computational Genetics, BCBB, DIR, NIEHS; Office of Scientific Computing, DIR, NIEHS; Office of Data Science, DNTP, NIEHS; Clinical Research Branch, DIR, NIEHS; Department of Biostatistics, University of Kentucky College of Public Health

Detecting gene by environment interactions (GxEs) for diseases enriches the ontology of genetic effects and helps identify environmental targets for interventions with the goal of improving health outcomes. However, the combined dimensions of genome and exposome poses challenges in terms of both computational and statistical power. The additive and multiplicative variance quantitative trait loci (vQTL) analysis has recently received attention for their ability to find candidate genome variants for GxEs without actual environmental exposome profiling. The rationale is that GxE unaccounted for by a genome-wide association study (GWAS) causing the residual variance of a quantitative trait changing across allele dosages—a non-uniformity capturable by a second GWAS treating the spread of residuals as a new phenotype. However, the vQTL approach is inefficient when the environmental direct effect on the phenotype is weak, and unable to identify GxE candidates for binary phenotypes. We propose variance loci analysis (VLA) as an improvement over current existing vQTL approach. We demonstrate that VLA can identify GxE candidates under weak direct environmental effect, and more importantly, by appropriately adjusting covariates, VLA can identify GxE candidates for thousands of binary phenotypes. To argue for our preference of additive over multiplicative vQTL as the basis of improvement, we show that the later being a sub-optimal selector for the current mainstream GxE model. We performed VLA for 3,273 health- and disease-related phenotypes derived from the UK Biobank and ranked the potential involvement of each variant in GxEs, and present the results in an outward facing catalog at genelist.niehs.nih.gov. Using environmental exposome data collected in the Personalized Environmental Genetic Study (PEGS), we found that high-ranking genome variants selected by VLA enriched the detection of genome-exposome-wide significant GxE SNPs for cardiovascular disease (CVD), type 2 diabetes (T2D).

Oral Presentation 4

Air pollution and breast cancer: an examination of modification by underlying familial breast cancer risk

Niehoff NM, Terry M, Bookwalter DB, Kaufman JD, O'Brien KM, Sandler DP, and White AJ

Environment & Cancer Epidemiology, Chronic Disease Epidemiology, EB, DIR, NIEHS
Department of Epidemiology, Mailman School of Public Health, Columbia University, Westat, Durham, NC,
Department of Environmental and Occupational Health Sciences, Medicine, and Epidemiology, University of Washington

Background: An increased familial risk of breast cancer may be due to both shared genetics and environment. Women with a family history of breast cancer may have a higher prevalence of breast cancer-related gene variants and thus may have increased susceptibility to environmental exposures. We evaluated whether associations between air pollutants and breast cancer varied by familial risk.

Methods: Sister Study participants living in the contiguous U.S. at enrollment (2003-2009) (N=48,453), all of whom had at least one first-degree relative with breast cancer, were followed for incident breast cancer. Annual NO2, PM2.5, and PM10 concentrations were estimated for the enrollment addresses. We predicted 1-year familial breast cancer risk using the Breast and Ovarian Analysis of Disease Incidence and Carrier Estimation Algorithm (BOADICEA). Using Cox regression, we estimated hazard ratios (HRs) and 95% confidence intervals (CIs) for associations between each pollutant and breast cancer with interaction terms to examine modification by BOADICEA score.

Results: NO2 (> vs. ≤median, 9.1ppb) was associated with a higher breast cancer risk among those with BOADICEA score >90th percentile (HR=1.28; 95% CI: 1.05-1.56) but not among those with BOADICEA score ≤90th percentile (HR=0.98; 95% CI: 0.90-1.06) (*p*-interaction=0.01). For PM2.5, women with >median BOADICEA score had an elevated risk of premenopausal breast cancer (HR=1.38; 95% CI: 0.97-1.96), whereas those at ≤median BOADICEA score did not (HR=0.96; 95% CI: 0.80-1.16) (*p*-interaction=0.07).

Conclusions: Our results provide additional evidence that air pollution may be implicated in breast cancer etiology, particularly among women who have a higher underlying familial risk.

Oral Presentation 5

Novel insights into the structure, function, and regulation of human tRNA splicing

Hayne CK, Stewart ZD, Butay KJ, Borgnia MJ, and Stanley RE
Nucleolar Integrity, STL, DIR, NIEHS

Transfer RNAs (tRNAs) are critical for translation, essential for life, and are regulators of cellular responses to stress. Like other RNAs, tRNAs require extensive modifications, including for many tRNAs, the removal of introns by the tRNA splicing endonuclease complex (TSEN). Mutations in TSEN and its established accessory factor, polyribonucleotide 5'-hydroxyl-kinase (CLP1), are associated with pontocerebellar hypoplasia (PCH), a family of incurable neurodevelopmental and neurodegenerative disorders. How each of the mutations in the TSEN proteins and CLP1 cause PCH remains poorly understood. A major barrier to understanding these proteins in the context of disease remains a lack of understanding about their underling essential cellular functions, which may include additional RNA substrates which have yet to be identified in metazoans. Until recently, it was believed that the TSEN complex requires CLP1 for support to remove introns from intron-containing pre-tRNAs. I reconstituted the human TSEN complex in a CLP1 free system, *E.Coli*, and showed that the TSEN complex does not require CLP1 to function *in vitro*. Further, we found that through its polynucleotidekinase activity, CLP1 is responsible for regulating the production of tRNA intronic circular RNAs (tricRNAs) and mature tRNA. We believe CLP1 is a critical regulator of tricRNAs, which may be toxic to cells. Using CryoEM, I am working to refine a high resolution structure of the TSEN complex bound to an intron containing pre-tRNA, revealing how the complex engages tRNA substrates and helping us better understand how mutations may be linked to TSEN assembly and regulation. In particular, we are able to see that all PCH-linked mutations in the TSEN complex and CLP1 are in regions outside the active sites and often on interfaces that may regulate not only TSEN assembly, but also the binding of regulatory proteins. I see that PCH mutations have minimal impacts on complex assembly and function *in vitro,* while having variable impacts on tricRNA production *in vivo*. These findings raise the question if the PCH mutations might also impact RNA processing of other unknown TSEN and CLP1 substrates. I currently working to understand what constitutes a TSEN substrate to better understand the role improperly processed RNAs may play in neuron death. I look forward to sharing my many recent unpublished results with the NIEHS audience.

Oral Presentation 6

Toll-Like-Receptor 5 Protects Against Pulmonary Fibrosis by Reducing Lung Dysbiosis

Sakamachi Y, Solis A, Johnson CG, Meng X, Hussain S, O'Dwyer DN, Mehta S, Trempus CS, Thomas SY, Li J, Zhou L, Karmaus PW, McGrath JA, Lipinski JH, Gibson K, Kass DJ, Gleiberman A, Walts A, Invernizzi R, Molyneaux PL, Yang IV, Zhang Y, Kaminski N, Schwartz DA, Gudkov AV, Garantziotis S

Matrix Biology, IIDL, DIR, NIEHS; University of Michigan, Ann Arbor; Social and Scientific Systems, Inc.; University of Pittsburgh Medical Center; Genome Protection Inc, Buffalo, NY; National Heart and Lung Institute, Imperial College, London, UK; University of Colorado School of Medicine; Yale University School of Medicine; Roswell Park Comprehensive Cancer Center, Buffalo, NY

Idiopathic pulmonary fibrosis (IPF) is a fatal and incurable lung disease with a mean survival of 3-5 years from diagnosis. Recently, microbial dysbiosis (imbalance in microbial community that is associated with disease) was found to be associated with IPF in human patients and in experimental animal models of fibrosis. Despite the emerging evidence of dysbiosis in IPF, genetic factors regulating the microbiota, in the context of IPF, are yet to be described.

Toll-like-receptor 5 (TLR5) is a pattern-recognition receptor for bacterial flagellin. In the present study, we have determined that carriers of a dysfunctional TLR5 allele, rs5744168, are susceptible to dysbiosis and IPF based on a cohort of 1133 patients and 2903 control subjects.

Congruently, *Tlr5*-deficient mice were susceptible to pulmonary fibrosis after bleomycin administration compared to wildtype littermates, while the pharmacological activation of TLR5 protected against bleomycin-induced fibrosis. Mechanistically, RNA sequencing revealed the upregulation of antimicrobial gene sets in TLR5-agonist-treated lungs, suggesting that TLR5 may protect against dysbiosis, an upstream event preceding fibrosis. Indeed, *Tlr5*-deficient mice displayed increased lung dysbiosis after bleomycin administration compared to wildtype littermates. Antibiotic treatment ameliorated fibrosis in *Tlr5*-deficient mice, suggesting that the protective effect of TLR5 is dependent on the presence of microbiota.

In conclusion, we have identified a novel susceptibility factor for IPF that functions by modulating the microbiome. Moreover, TLR5 agonism represents a novel therapeutic approach to treat IPF and may have wider implications for non-antibiotic antimicrobial treatment in a variety of diseases associated with dysbiosis.

Oral Presentation 7

Poly(A) tail dynamics during cell differentiation show transcript compartmentalization and specific post-transcriptional regulation

Baptissart M, Papas B, Puviindran B, Li Y, and Morgan M
Male Reproduction and RNA Biology, RDBL, DIR, NIEHS, Integrative Bioinformatics Support Group, DIR, NIEHS

Changes in poly(A) tail length influence mRNA stability and ultimately define the transcriptome composition. The typical poly(A) tail of a transcript is around 60 nucleotides (nts) long, with poly(A) tail shortening below 30-nt triggering 3' uridylation and decay. However, during germ cell differentiation, the poly(A) tail of some key transcripts have been shown to shift between 60 and more than 100-nts long. This interesting observation raises fundamental questions: 1) Is this dynamic present also during the differentiation of somatic cells? 2) Is this unique to a handful of transcripts or operates at the population level? 3) Is this dynamic functionally associated with variations in mRNA accumulation observed through differentiation? To answer these questions, we tracked changes in global poly(A) tail profiles, using long-read sequencing technologies, in a model of in vitro neuronal differentiation. In undifferentiated cells, we identified, in addition to the typical 60-nts poly(A) tail length population, an abundant population of mRNAs with tails 120-nts long. As the cells differentiate into neurons, the frequency of transcripts with 120-poly(A) length gradually decreases. Interestingly, this dynamic is specific to RNAs downregulated upon differentiation which also show a significant acceleration of their decay rates. In contrast, upregulated transcripts show no significant changes in their decay rates together with a unique 60-nts long poly(A) tail profile that does not change during differentiation. To understand the mechanisms of this selective decay acceleration, we focused on the Terminal Uridyl-Transferases TUT4 and TUT7 (TUT4/7), two enzymes known to enhance mRNA degradation. We found that TUT4/7 are critical to establish a functional transcriptome since their depletion leads to an early arrest of neuronal differentiation. During this process, the upregulated transcripts appear to be the only population of mRNAs insensitive to TUT4/7-mediated uridylation, which could in part explain their enhanced stabilization. Overall, we show that the transcriptional program of differentiation is driven by unique poly(A) tail dynamics, providing differential stability to selected groups of mRNAs. Studying the mechanisms underlying the compartmentalization of tail processing is critical to understand the origin of differentiation-associated diseases such as cancer or infertility.

Oral Presentation 8

Serum and urine profiles of TGF-β superfamily members in reproductive age women

Calvert ME, Kalra B, Patel A, Kumar A, and Shaw ND
Pediatric Neuroendocrinology, CRB, NIEHS
Ansh Labs LLC, Webster, TX

Background: There has been a growing clinical interest in measuring ovarian and placental TGF-β superfamily members as markers of reproductive health. Activins, inhibins, and follistatin, for example, are granulosa cell byproducts that control follicle growth and FSH secretion. Anti-Mullerian hormone (AMH), another TGF-β granulosa cell protein, inhibits primordial follicle growth and antral follicle recruitment. Growth differentiation factor-9 (GDF-9) and bone morphogenetic protein-15 (BMP-15) are oocyte-derived proteins that function as a heterodimer and control granulosa cell survival, function, and maturation. Lastly, growth differentiation factor-15 (GDF-15) is a TGF-β family cytokine highly expressed in placental trophoblast cells. Its primary function is unknown but levels are altered in pre-eclampsia, and genetic variants in *GDF-15* are associated with an increased risk of hyperemesis gravidarum. While a number of these proteins have been measured in serum, there have been very few attempts to measure them non-invasively, such as in urinary samples.

Methods: Paired serum and urine samples were collected from healthy reproductive age women and pregnant (second trimester) women and assayed for inhibin A, inhibin B, total inhibin, AMH, activin A, activin B, activin AB, follistatin, the GDF-9/BMP-15 complex, and GDF-15.

Results: All biomarkers were detected in serum in both pregnant and non-pregnant women. GDF-15 was the only hormone consistently detected in urine. Pregnant women had significantly higher serum levels of inhibin A (mean ± SE: 257.6 ± 70.9 vs. 26.2 ± 5.5 pg/mL in pregnant vs. non-pregnant, $p < 0.0001$), total inhibin (228.7 ± 40.6 vs. 69.4 ± 10.8 pg/mL, $p < 0.0001$), activin A (2.2 ± 0.4 vs. 0.5 ± 0.1 ng/mL, $p < 0.0001$), activin AB (7.8 ± 0.9 vs. 4.5 ± 0.5 pg/mL, $p=0.0005$), follistatin (8.0 ± 1.1 vs. 1.5 ± 0.2 ng/mL, $p<0.0001$), and GDF-15 (233.5 ± 4.8 vs. 14.9 ± 1.4 pg/mL, $p<0.0001$) than non-pregnant women, whereas serum inhibin B, AMH, activin B, and GDF-9/BMP-15 levels did not vary by pregnancy status. Serum and urinary GDF-15 levels largely fell in the low to mid-200 pg/ml range.

Conclusion: All reproductive peptides, including the GDF-9/BMP-15 heterodimer complex, were successfully detected in serum; only GDF-15 could be reliably measured in urine. Previous studies have detected the isolated forms of GDF-9 and BMP-15 in serum; here we report for the first time, serum levels of the functional GDF-9/BMP-15 heterodimer. Consistent with previous studies, inhibin A and total inhibin, activin A and total activin, follistatin, and GDF-15 were detectable in serum and levels were significantly higher in pregnant than non-pregnant women. As GDF-15 levels have been reported to be altered in the serum of women with an ectopic pregnancy, pre-eclampsia, gestational diabetes, or at increased risk for miscarriage, urinary GDF-15 levels may serve as an important non-invasive biomarker for tracking the health of the mother and fetus during pregnancy.

Oral Presentation 9

Engineering Human Neural Organoids to Explore Developmental Neurotoxicity Induced by Chronic Arsenic Exposure

Wu X, Dixon D, and Tokar EJ
Stem Cell Toxicology, MTB, DNTP, NIEHS

Modeling brain development and function is challenging due to the complexity of the organ. Recent advances in human pluripotent stem cell (PSC)-derived brain-like organoids provide new tools to study the human brain. These 3D models together with 2D cellular assays have the potential to enhance our understanding of the mechanisms of developmental neurotoxicity (DNT) during the early stages of neurogenesis and offer a rapid, cost-effective approach for assessing chemical safety. Arsenic (As) is a widespread environmental contaminant. Exposure to As is associated with DNT-related diseases. However, mechanisms of As-induced DNT are not well-defined. Here, we used 3D PSC-derived embryoid bodies (EBs) to recapitulate events involved in early embryogenesis and neurogenesis before neural induction, and EB-derived neural organoids to mimic neural development in vivo. A 7-day exposure to a human-relevant, non-cytotoxic dose (0.5 μM; 35 ppb) of As increased ectoderm differentiation within the EBs through upregulated expression of *PAX6, SOX1, COL2A1*, all of which play critical roles in early embryonic development. Histological staining of As-treated EBs showed neural rosette structure disruption. Organoids showed VIMENTIN+ astrocytes and NESTIN+ neural SCs, confirming cerebral phenotype. Ingenuity pathway analysis (IPA) of RNAseq data from organoids indicated CREB signaling was activated in the neural induction stage and enhanced during neural maturation (day 7 to day 40) while pluripotency signaling was suppressed. The IPA-identified top 5 pathways affected by As treatment were CREB signaling in neurons, neuronal synapse pathway, GABA receptor pathway, synaptogenesis signaling and axonal guidance signaling. GO enrichment analysis found G-protein signaling on the cell membrane was suppressed and WNT, Notch, and FGF signaling pathways were all inhibited by As treatment. RNAseq analyses were confirmed by real-time qPCR, which also found As-inhibited expression of markers for mature neural cells (*MAP2, vGLUT2*) and astrocytes (*GFAP*). Inhibition of neuronal gene expression was also confirmed in a neurite outgrowth 2D morphology assay that mimics nerve growth and axon pathfinding in vivo and in the disrupted neural rosette and neuropil structures in day 40 organoids. In conclusion, the results described herein show that this EB and neural organoid 3D model system can provide valuable insights into the cellular events and molecular mechanisms of As-induced DNT.

Oral Presentation 10

How asymmetric DNA replication achieves high and symmetrical fidelity

Zhou Z, Lujan SA, Burkholder AB, St. Charles J, Dahl J, Farrell CE, Williams JS, and Kunkel TA

DNA Replication Fidelity, GISBL, DIR, NIEHS and Integrative Bioinformatics Support Group, DIR, NIEHS

Eukaryotic genome replication presents inherently asymmetric challenges. Nascent leading and lagging DNA strands have different structures and are synthesized by different polymerases. Accurate DNA synthesis depends on selectivity for matched nucleotides, exonucleolytic proofreading of mismatches, and removal of remaining mismatches via DNA mismatch repair (MMR). Defects in any of the three processes are highly associated with tumorigenesis. Yet how these processes cooperate *in vivo* is not fully understood. Replicative DNA Polymerases (Pols) α, d, and e are highly selective. Pols d and e also have 3′-5′ exonucleases into which mismatches are partitioned for proofreading *in cis* (intrinsic proofreading). During intrinsic proofreading, mismatches made at polymerase active sites are transferred to the exonuclease active site for removal without enzyme dissociation. Pol d is also proposed to extrinsically proofread mismatches that are initially abandoned after misincorporation. Here we provide strong evidence that Pol d can extrinsically proofread mismatches made by itself and those made by Pol e. We show that extrinsic proofreading can occur independently of Pol d's polymerization activity and independently of its proposed role in MMR. We show that extrinsic proofreading across the budding yeast genome is remarkably efficient, and that its specificity differs from intrinsic proofreading, in part due to differences in the ability of synthesizing polymerase to extend various mismatches. We report, with unprecedented accuracy, *in vivo* contributions of nucleotide selectivity, proofreading and mismatch repair to the fidelity of leading and lagging strand DNA replication, and uncover multiple lines of critical information. We show that the ability of Pol d to extrinsically proofread mismatches improves and balances the fidelity of replication of the two DNA strands. Together, for the first time, we depict a comprehensive picture how nucleotide selectivity, proofreading and MMR cooperate to achieve high and symmetrical fidelity on the two strands.

Poster Presentation 1

Neighborhood social cohesion and obesity across racial/ethnic groups in the United States

Al-Hasan DM, Gaston SA, Jackson II B, and Jackson CL
Social & Environmental Determinants of Health Equity Group, DIR EB, NIEHS, Social & Scientific Systems, Inc., a DLH Holdings Company,

Prior research has shown that low neighborhood social cohesion (nSC) is associated with obesity, but few studies have assessed the nSC-obesity relationship among a large, racially/ethnically diverse, and nationally representative sample of the United States population. We examined overall and race/ethnic-specific cross-sectional associations by age among 149,965 participants of the National Health Interview Survey from 2013-2018. Based on a 4-item scale from the Project on Human Development in Chicago Neighborhoods Community Survey, we categorized nSC as low, medium, and high. We categorized obesity as a body mass index ≥30 kg/m2 vs. non-obese (<30 kg/m2). We used Poisson regression with robust variance to estimate PRs and 95% CIs while adjusting for sociodemographics (e.g., annual household income, educational attainment and marital status) and other confounders. Mean age± standard error of study participants was 47.1±0.1 years, most (69.2%) self-identified as Non-Hispanic (NH)-White and 51.0% were women. Among NH-Whites, a lower percent lived in low (61.8%) vs. high (77.0%) nSC. A higher percent of NH-Black and Hispanic/Latinx participants reported low (14.0%; 19.1%) vs. high nSC (7.7%; 10.4%), respectively. Low vs. high nSC was associated with a 14% higher prevalence of obesity (PR=1.14 [95% CI: 1.11-1.17]), and the magnitude of the association was stronger among NH-White (PR=1.19 [95% CI: 1.15-1.23]) than Hispanic/Latinx (PR=1.03 [95% CI: 0.96-1.10]) and NH-Black (PR=1.01 [95% CI: 0.95-1.07]) adults. Among NH-White adults, low vs. high nSC was associated with a 20% higher prevalence of obesity among adults ≥50 years old (PR=1.20 [95% CI: 1.16-1.25]) compared to <50 years old (PR=1.12 [95% CI: 1.07-1.18]). Among Hispanic/Latinx adults, low vs. high nSC was associated with obesity among ≥50 years old (PR=1.14 [95% CI: 1.02-1.28]) but not <50 years old (PR=0.95 [95% CI: 0.87-1.03]) adults. Enhancing nSC may improve health and address health disparities.

Poster Presentation 2

Control of dNTP Pools and Their Role in Genome Integrity

Alagna NS, and Schaaper RM
Mechanisms of Mutation, , NIEHS, Mechanisms of Mutation, GISBL, DIR, NIEHS

The relative and absolute levels of the four canonical DNA precursors have been shown to significantly impinge upon the occurrence of mutational events during DNA replication. As such, cells feature a host of genes and associated pathways that function to tightly regulate the quantities of these four nucleotides. Our lab has previously revealed that the *Escherichia coli dgt* and *nrdR* genes, both of which have a role in dNTP metabolism, exert a substantive influence over the fidelity of DNA synthesis. When one or both of these genes were knocked out, hypermutability was induced. Relative to the wild-type, the *dgt* strain exhibited a 2-fold increase in mutation frequency, while the *nrdR* and *dgtnrdR* strains had a 3-fold and 19-fold elevation, respectively. In the present study, we sought to demonstrate the relationship between the mutation frequencies in the strains of interest and their intracellular dNTP levels, by quantitating the nucleotide pools from cellular extracts using IPRP-HPLC. Data from extracts derived from actively growing cells show an elevation in dGTP and dTTP in the *dgt* strain and an increase in all four DNA precursors in the *nrdR* and *dgtnrdR* strains. These results support our putative idea that the heightened mutagenicity in these strains is due to aberrant, imbalanced dNTP pools.

Poster Presentation 3

Potential role of serotype and perineuronal nets in the preferential expression of adeno-associated virus-packaged genetic cargo in hippocampal CA2 neurons

Alexander GM, Carstens KE, Gloss B, Lilly SR, Slay BS, Martin NP, and Dudek SM
Synaptic and Developmental Plasticity, DIR NL, NIEHS,

A common approach to studying brain circuits is through viral delivery of genetic material that encodes effector molecules and fluorophores. This is often accomplished through direct injection of adeno-associated viral (AAV) particles into the target brain area, or via the bloodstream for some serotypes. In previous studies of hippocampus and in our own experiments in hippocampus, we have observed preferential expression of AAV-delivered cargo in the CA2 subfield compared to neighboring CA1 and CA3, even when injections do not target CA2. This curious observation led us to ask why CA2 neurons are preferentially targeted by AAVs. Because different AAV serotypes target different receptors, one possible mechanism by which differential AAV expression occurs is that CA2 neurons may preferentially express a receptor for specific serotypes of AAVs. Thus, we predicted that preferential expression of AAVs by CA2 neurons would vary with different serotypes, which target different receptors. Alternatively, we hypothesized that the preferential targeting of AAVs to CA2 is mediated by the dense expression of a specialized extracellular matrix, perineuronal nets (PNNs), which uniquely surround excitatory CA2 pyramidal neurons in addition to specific populations of inhibitory neurons throughout the brain.

To test the hypothesis that AAV expression in CA2 is dependent upon serotype, we injected AAVs of various serotypes, each coding for green fluorescent protein (GFP) under the control of the human synapsin (hSyn) promotor, into the hippocampus of C57Bl/6 mice. Thus far, we have found that for each of multiple AAV serotypes injected intra-hippocampally, CA2 neurons preferentially express GFP relative to CA1 and CA3 neurons. In addition, we found that GFP was preferentially expressed in CA2 neurons after retro-orbital injection of the PHP.B serotype, which is known to cross the blood-brain barrier. To address the role of PNNs in AAV infection, we generated a conditional aggrecan gene (*ACAN*) knock-out (KO) mouse. Aggrecan is a primary component of PNNs detected around CA2 neurons as well as a class of interneurons. By pairing this “floxed” *ACAN* strain with our CA2-targeted *Amigo2* cre strain or parvalbumin (PV) neuron-targeted cre strain, we successfully deleted *ACAN* and thus detection of PNNs from CA2 pyramidal neurons or from PV neurons, respectively. We injected CA2 *ACAN* KO mice with PHP.B-hSyn-GFP retro-orbitally and found that despite the absence of PNNs, CA2 neurons continued to express GFP. These data do not support the hypotheses that preferential expression of AAVs by CA2 varies according to AAV serotype or that PNNs (or at least *ACAN*), is required for preferential expression in CA2 and point toward an alternative mechanism.

Poster Presentation 4

A hindlimb derived cell population is necessary in penis formation

Amato CM, and Yao HH
Reproductive Developmental Biology, DIR RDBL, NIEHS,

Hypospadias, or incomplete closure of the urethra along the penis, is the second most common birth defect in the United States. This defect often requires surgical correction and if not corrected, it can lead to difficult urination and intercourse, leaving lasting physical and psychological impacts. In the male embryo, the urethra first starts to close at the base of the penis. This closure continues up the penis in a zipper-like fashion where it eventually forms a tube along the length of the penis. Disruption at any time during the closure event results in hypospadias. Therefore, understanding penis development has significant implications on human health. Here we report a population of mesenchymal cells responsible for proper penile urethra closure in the mouse. After the onset of penis formation, a population of mesenchymal cells appears near the hindlimb of the fetus. Just prior to urethra closure initiation, these hindlimb-derived cells migrate centrally and gradually positioned bilaterally to the penile urethra. Using single cell RNA sequencing, we discovered that these hindlimb-derived cells express markers of hindlimb development and secreted factors that drive urethra formation. Removal of the hindlimb-derived cells, using a cell-type specific ablation model, resulted in severe urethra closure malformations. In many cases there was a failure to initiate the closure of the urethra. Our results reveal hindlimbs as a source mesenchymal cells in the penis that are required for the initiation of urethra closure. These hindlimb-derived cells provide new entry points to understand the biology of urethra closure and potential causes of hypospadias in humans.

Poster Presentation 5

DNA Ligase 1: Ligation, Fidelity and a Role In Maintaining Genome Stability

Arana ME, Williams JS, Tumbale PP, Rana J, Williams SR, and Kunkel TA
DNA Replication Fidelity, DIR GISBL, NIEHS, Structural Cell Biology, DNA Replication Fidelity

During nuclear DNA replication of leading and lagging strands, accurate nucleotide and sugar selectivity by the replicative DNA polymerases α, δ and ε are of utmost importance. DNA ligases are essential enzymes for DNA replication and repair pathways. Following the completion of synthesis, DNA ligase 1 joins the DNA strands to complete DNA replication, preserving genome integrity. This process occurs ~50,000,000 times in human cells during the maturation of Okazaki fragments to complete replication of the lagging strand. Recent work by Tumbale *et al*. (2019) presented a high-resolution X-ray structure of human DNA ligase 1 (LIG1) bound to a nicked DNA duplex. This structure revealed an additional Mg^{2+} ion, that reinforces DNA binding which is critical to establishment of a high-fidelity (Hi-Fi) interface between LIG1, Mg^{2+} and the DNA substrate. This interaction involves two highly conserved glutamic acid residues in LIG1. Biochemical studies show that mutation of these two glutamic residues to alanine creates an enzyme with lower fidelity, with the loss of Mg^{2+} coordination in the EEAA mutant protein creating an open cavity in the enzyme that allows accommodation and sealing of damaged termini in a nicked DNA substrate.

These results prompted us to test the importance of DNA ligation fidelity in vivo by constructing a *Saccharomyces cerevisiae* strain expressing the equivalent EE to AA mutations in Cdc9, the yeast LIG1 homologue, and measuring spontaneous mutation rates and specificity. We observe an elevated rate of +1 insertions in homopolymeric runs in the cdc9-EEAA mutant. We extended this analysis by inactivating either DNA mismatch repair (MMR) or the FEN1 endonuclease important for Okazaki fragment maturation by deleting the genes encoding *MSH2* or *RAD27*, respectively, in the *cdc9-EEAA* strain. The rate of +1 insertion events was further elevated in both the *cdc9-EEAA msh2⊿* and *cdc9-EEAA rad27⊿* double mutants, supporting the import role of DNA ligase 1 in maintaining fidelity during ligation of Okazaki fragments to complete lagging strand replication. Consistent with these mutational analyses, here we present structural and biochemical evidence that the *cdc9-EEAA* mutant protein is capable of mutagenic DNA ligation by accommodating an additional base upstream of its active site. These results demonstrate that the fidelity of ligation by DNA ligase 1 is achieved through coordination of theHi-Fi Mg^{2+}. High fidelity DNA ligation is critical for preventing +1 insertion mutagenesis *in vivo*.

Poster Presentation 6

Structure-Function Analysis of the Herpes Simplex Virus-1 Primosome

Bermek O, and Williams SR
Genome Stability Structural Biology, DIR GISBL, NIEHS,

Herpes simplex virus type 1 (HSV-1) is one of the nine herpesviruses that infect humans. HSV-1 encodes its own proteins to replicate its genome in the hijacked human cell. In the HSV-1 replisome, the helicase-primase complex is comprised of three components including UL5 (helicase), UL52 (primase) and UL8 (non-catalytic subunit). The primary amino acid sequences of UL5 and UL52 are highly conserved amongst all herpesviruses. Thus, compounds inhibiting the helicase/primase complex could be used as a broad-spectrum drug. However, we lack a structural and molecular understanding of the helicase/primase complex of HSV-1 or any other herpesvirus. Towards solving the atomic resolution structure, we established a robust protein expression system to obtain the trimeric helicase-primase complex in milligram quantities. Using a 3-gene MacroBac baculovirus significantly increased the expression level of the protein complex. We purified the protein as a stable complex where the subunits are associated with a ~1:1:1 stoichiometry.

The UL8 subunit has a central role in coordinating UL5 and UL52, UL8 alone forms filamentous structures on single-stranded M13 DNA. We obtained promising results of the structure of the nucleoprotein complex using cryo-EM. These filaments are very different than the usual DNA-protein helical filaments. Tilted cryo-EM single-particle analysis is being used to resolve the orientation bias. Preliminary analysis from molecular modeling indicates that UL8 forms ring shaped structures. Further studies are in progress to analyze the inter-subunit interactions. A BS3 crosslinking approach is also being used to improve the conditions for cryo-EM as the protein has the propensity to form aggregates. We aim to further stabilize the complex using nucleic acids such as forked DNA substrates as such interaction is confirmed by our EMSA studies.

In conclusion, we built a solid foundation towards solving the structure of HSV-1 helicase/primase complex. At the present time, we are working on improving the conditions for the high resolution of the three-dimensional structure of the HSV-1 helicase/primase complex.

Poster Presentation 7

Characterizing fetal growth trajectories among small-for-gestational age births in the LIFECODES Birth Cohort

Bommarito PA, Cantonwine DE, McElrath TF, and Ferguson KK
Perinatal and Early Life Epidemiology, DIR EB, NIEHS, Brigham and Women's Hospital, Harvard Medical School,

Background: Fetal growth restriction (FGR) is associated with adverse health outcomes, both at delivery and later in life. There is no gold-standard diagnostic criteria for FGR. In population-based studies, small-for-gestational age (SGA; birthweight < 10th percentile) at birth is used as a proxy for FGR.

Objective: Improve upon identification of FGR births by incorporating ultrasound measures of fetal growth.

Results: We characterized trajectories of fetal growth among SGA babies (N = 242) in the LIFECODES Fetal Growth Study using univariate and multivariate trajectory modeling approaches. We abstracted ultrasound measures of fetal growth (estimated fetal weight [EFW], head circumference [HC], abdominal circumference [AC], and femur length [FL]) from health records. First, we applied univariate group-based trajectory modeling to define trajectories of EFW during gestation. Second, we applied group-based multi-trajectory modeling to identify trajectories based on concurrent measures of HC, AC, and FL. Last, we described how these trajectories to demographics, pregnancy characteristics, and available birth outcomes. We identified three unique univariate trajectories and four unique multivariate trajectories of fetal growth. In both approaches, infants that remained small throughout pregnancy had the worst outcomes. In our multi-trajectory modeling approach, we also identified a set of infants with birthweights similar to other SGA babies, but with greater rates of NICU admission.

Discussion: Trajectory modeling applied to ultrasound measures of fetal growth may help distinguish pathologic vs. constitutional smallness among babies born SGA.

Poster Presentation 8

The Potential Role of Runx1 in Ovarian Cancer and Pathologies

Bridges KA, Nicol B, and Yao H
Reproductive Developmental Biology, DIR RDBL, NIEHS,

Runt-related transcription factor 1 (RUNX1) is a transcription factor that is involved in the regulation of cell fate determination and lineage differentiation. Previous findings identified RUNX1 as a regulator in securing the identity of ovarian-supporting cells and the ovary. Considering its role in ovarian development, we set up to investigate how changes in the expression of the gene *RUNX1* are linked to ovarian dysfunction. Several modifications in *RUNX1* have been associated with ovarian cancer cases in humans, such as the deletion of *RUNX1* and the amplification of *RUNX1*. We therefore developed two mouse models that mimic these two genetic alterations that are associated with ovarian cancer. We first focused on the effects of the loss of *Runx1* in the mouse ovary by generating a conditional knockout (KO) of *Runx1* where the gene was removed in somatic cells expressing Steroidogenic factor 1 (SF1). We collected ovaries of control and *Runx1* KO at 4.5- and 15-month-old and characterized their phenotypes by histology, immunostaining using a panel of markers and gene expression analyses. The results at the 4.5 months revealed the occurrence of abnormal, asymmetrical ovarian follicles in the *Runx1* KO mice but not in the control mice. These abnormal follicles lacked signs of cell proliferation or apoptosis, suggesting that these follicles remain quiescent at this time. Several genes previously demonstrated to be involved in tumor progression are altered in Runx1 KO mice. RNA-Sequencing analysis led to the identification of differentially expressed genes in Runx1 KO ovaries, including genes involved in ovarian cancer. At 15 months of age, about one third of *Runx1* KO mice developed ovarian masses. We are currently examining the molecular pathways that are affected by the loss of RUNX1 and developing the *Runx1* overexpression model. Understanding how certain genes play a role in cancer will enhance our ability to overcome the challenges of early detection, develop therapeutic strategies and help in improving the survival of the patients.

Poster Presentation 9

A human pluripotent stem cell-based high-throughput platform with artificial intelligence technology to screen for developmental toxicants

Chen I, Birla S, and Tokar E
Mechanistic Toxicology Branch, DNTP, NIEHS, Research Triangle Park, NC 27709, USA,

Environmental factor-induced birth defects raise the risk for lifelong disabilities to survivors and increase the economic burden to their families and society. While over 80,000 chemicals are registered for use in the United States, many of them have undergone little safety testing. Therefore, a rapid and accurate method for predicting developmental toxicants to humans is desired. Here, we developed a human pluripotent stem cell (hPSC)-based high-throughput platform with artificial intelligence technology to screen for developmental toxicants. Embryoid bodies (EBs) generated from hPSCs were used since their formation recapitulates early embryogenic processes. A two-part toxicity prediction system was built upon the transcriptional response and morphological change of EBs to 35 chemicals with confirmed teratogenicity in humans and experimental animals. The expression change of 20 hallmark genes of embryogenesis was subjected to machine learning with 10 different algorithms. With feature selection, the Random Forest-based classification model showed a good accuracy (53%) to categorize the 35 chemicals correctly into four different risk levels (none, minimal, moderate, and high), forming the first part of the prediction system. The second part of the system is based on chemical-elicited structural alterations in EBs, captured by high-content fluorescent imaging with germ layer-specific markers (TUJ1 for ectoderm, SMA for mesoderm, and SOX17 for endoderm). A highly accurate (81%) prediction model based on DenseNET deep learning technology was obtained through training with 31,644 EB images from each chemical. To further validate the prediction accuracy and prove the practical value of this screening system, the teratogenicity of an additional 20 chemicals with limited toxicity information was assessed by this platform and the results were consistent with previous studies. Tretinoin, as an example, was classified as a ‘high’ risk teratogen to humans by both subordinary prediction models and showed a 34% toxicity similarity with Etretinate, a confirmed teratogen from the same vitamin A derivative family. Sucrose was classified as ‘nonteratogenic’ as it showed a 47% similarity to ascorbic acid on EB formation. Together, these results present a promising capability of our screening platform in identifying human developmental toxicants and understanding their etiology.

Poster Presentation 10

WNK1 is vital for male fertility through regulating both meiotic initiation and progression during spermatogenesis

Chi RA, Xu X, Li J, Kirsanov O, Geyer C, Xu X, Willson C, Hu G, Huang C, and DeMayo F

Pregnancy & Female Reproduction, DIR RDBL, NIEHS, Integrative Bioinformatics, NIEHS, National Institutes of Health, Research Triangle Park, NC, USA., East Carolina Diabetes and Obesity Institute,

With No Lysine (K) Kinase 1 (WNK1) is a widely expressed kinase with tissue-specific functions in both humans and mice. Initially identified in connection with high blood pressure in humans, WNK1 is most well studied and understood as a regulator of ion homeostasis in the renal system. Little is known regarding WNK1's role in reproduction, and we have previously shown that in female mice, WNK1 is critical for maintaining proper uterine structure and embryo implantation. An unexpected discovery revealed that WNK1 is critical for spermatogenesis, and that loss of germline *Wnk1* expression caused male infertility. Spermatogenesis is a process whereby the spermatogonia undergo a series of differentiation to form meiotic spermatocytes. Completion of meiosis produces haploid spermatids, which further transform into elongated spermatids and are then released into the epididymis as testicular sperm. A detailed examination revealed that WNK1 is detectable in all spermatogenic cells. In addition, WNK1 was upregulated during the spermatogonia to spermatocyte transition, resulting in peak expression in preleptotene spermatocytes. To understand WNK1's spermatogenic function, we ablated *Wnk1* expression using two *Cre* models – the inducible *Ddx4-CreERT2* which is expressed in all spermatogenic cells; and *Wnt7a-Cre*, which is expressed in pachytene spermatocytes. Both *Ddx4-CreERT2* and *Wnt7a-Cre* mediated *Wnk1* deletion led to sterility with approximately 70% reduction in testicular size. Excitingly, the two mouse models exhibited different spermatogenic arrest. The *Wnt7a-Cre;Wnk1f/f* mice initiated meiosis but were unable to complete it, while the *Ddx4-CreERT2;Wnk1f/f* mice failed to initiate meiosis altogether. These findings revealed that WNK1 is an essential factor for both meiotic initiation and meiotic progression. Single-cell RNA-sequencing was next conducted on the control and *Wnt7a-Cre;Wnk1f/f* testes to understand how loss of *Wnk1* impacted the transcriptome in the meiotic cells. We found that expression of numerous mRNA translation factors was disrupted, including both translation initiation and elongation factors. As the germ cells' genome is inaccessible for transcription during multiple stages of spermatogenesis, translation becomes the main mechanism to control gene expression. Therefore, we speculate the possibility that the meiotic failure observed in the *Wnt7a-Cre;Wnk1f/f* mice was associated with disrupted translation. Supporting this, we found that WNK1 represses the master translation promoter mTORC1, and that loss of WNK1 led to elevated mTOR expression. This was functionally significant, as mTORC1 downstream translation mediators EIF4EBP1 and RPS6 both showed increased phosphorylation in the absence of WNK1. Taken together, we show that WNK1 is indispensable for male fertility via regulating multiple aspects of meiosis during spermatogenesis, and that it accomplishes this potentially through controlling mRNA translation.

Poster Presentation 11

GLIS3-Deficiency in the Maturing Kidney Leads to Metabolic Reprogramming and Polycystic Kidneys

Collier JB, Roh Y, Srivastava C, Kang H, Grimm S, and Jetten AM
Cell Biology, DIR IIDL, NIEHS,

Deficiency in the Krüppel-like zinc finger transcription factor (TF) GLI-Similar 3 (GLIS3) in both humans and mice leads to a rare syndrome with a multi-organ phenotype that includes neonatal diabetes, congenital hypothyroidism, and polycystic kidney disease (PKD). PKD is characterized by the chronic development of fluid-filled cysts in the kidneys and affects 4 to 7 million people worldwide. The cyst accumulation impairs renal function and leads to renal failure accounting for 7-15% of all renal replacement therapy with an estimated healthcare burden of $5.7 billion annually. To study the role of GLIS3 in the development of PKD we developed a GLIS3 knockout mouse (GLIS3KO). Transcriptome analysis of GLIS3KO and WT kidneys was performed on postnatal days 7, 14, and 28 to identify the regulatory pathways affected by the loss of GLIS3. Gene set enrichment analysis identified mitochondrial oxidative phosphorylation (OXPHOS) as the top negatively regulated process at P7, 14, and 28. Pathway analysis of differentially expressed genes showed significant downregulation of mitochondria-related pathways in GLIS3KO kidneys, including OXPHOS coupled production of ATP, electron transport chain, TCA cycle, and mtDNA transcription pathways. These findings were significant as the kidney is one of the most mitochondria-driven, metabolically active organs, and without GLIS3 the maturing kidney fails to properly regulate these required metabolic pathways. Additionally, using qPCR we observed in maturing WT kidneys the upregulation of mitochondrial TFs, TFAM, TFB1M, and TFB2M, and the level of mtDNA demonstrating a growing need for mitochondria metabolism, yet the GLIS3KO kidneys failed to upregulate these factors. ChIP-Seq identified GLIS3 binding in the promoter regulatory regions of TFAM, TFB1M, and TFB2M suggesting a direct regulation by GLIS3. To further elucidate the metabolic phenotype, GLIS3KO cultured primary renal tubule epithelial cells (RTEC) were run on an XF96 analyzer and a clear shift from mitochondrial OXPHOS to a more glycolytic phenotype was observed. Furthermore, the GLIS3KO primary cells were found to produce and export the metabolite lactate at higher rates than WT cells, implicating a metabolic reprogramming in the GLIS3KO kidney to an increased glycolytic phenotype similar to many cancer cells. Our study identified GLIS3 as a major TF that is vital for the proper mitochondrial metabolic upregulation in the maturing kidney. GLIS3 absence leads to a state of mitochondrial hypometabolism with a shift towards aerobic glycolysis which is contrary to physiological renal metabolism. This metabolic reprogramming initiates an environment conducive for cyst formation and growth. This novel GLIS3-metabolism association may lead to new insights and therapeutic approaches for the management of PKD.

Poster Presentation 12

Identifying Multivariate Latent Class Growth Trajectories via the Bayesian Tensor Mixture of Regressions Model

Davalos AD, Ferguson KK, and Zhao S
Applied Statistics, DIR BCBB, NIEHS, Perinatal & Early Life Epidemiology, DIR EB, NIEHS,

Identifying fetal growth trajectories from longitudinal ultrasound data can be an important epidemiological tool for linking unique growth patterns with exposures of interest and subsequent adverse health outcomes. Latent class methods have gained use in epidemiologic research for identifying trajectories of fetal growth, however, current methods for multivariate longitudinal data with large heterogeneity (i.e., many clusters) have interpretation difficulties. We consider a Bayesian tensor mixture of regressions framework for simultaneous clustering of the marginal and joint growth trajectories as an alternative. The clustering performance is compared to a current exploratory data analysis tool (i.e., group-based multi-trajectory modeling) via simulations. The proposed method is used to identify joint trajectories of fetal growth on ultrasonic measures of head and body size in a US birth cohort study.

Poster Presentation 13

A 14-day toxicity class comparison study of nine phenolic benzotriazoles in male Sprague Dawley rats

Dee RA, Blystone CR, Cora MC, Shockley KR, Stout MD, and Waidyanatha S
DNTP, NIEHS

Phenolic Benzotriazoles (PBZTs) are a class of UV stabilizers used in a variety of industrial and consumer products. Due to widespread use there is potential exposure to the general public, with limited class data available on these chemicals. The objective of this study was to evaluate and compare the general toxicity of nine PBZTs: 2-(2H-benzotriazol-2-yl)phenol (P-BZT), Drometrizole, 2-(2H-benzotriazol-2-yl)-4-tert-butylphenol (tBu-PBZT), Octrizole, 2-(2H-benzotriazol-2-yl)-4,6-bis(1,1-dimethylpropyl)phenol (ditPe-BZT), 2-(2H-benzotriazol-2-yl)-4,6-bis(1-methyl-1-phenylethyl)phenol (diMeEtPh-BZT), 3-(2H-benzotriazol-2-yl)-5-(1,1-dimethylethyl)-4-hydroxybenzenepropanoic acid, octyl ester (tBuPrOcEst-BZT), Bumetrizole, and 2-(5-chloro-2H-benzotriazol-2-yl)-4,6-bis(1,1 dimethylethyl)phenol (ditBu-ClBZT). The test article, or vehicle control, was administered daily to male Sprague Dawley rats via oral gavage for 14 days at dose levels of 0, 30, 100, 300, or 1000 mg/kg. No treatment-related mortality was observed. Animals exposed to 1000 mg/kg tBuPrOcEst-BZT displayed several clinical signs of toxicity, accompanied by significant changes in hematological and clinical chemistry parameters, suggestive of renal and hepatic injury. Animals exposed to high doses of tBu-BZT, ditPe-BZT, and ditBu-ClBZT also displayed significant changes in hematological and clinical chemistry parameters. Body weights were significantly decreased ($p<0.001$) by up to 34% in animals treated with ≥300 mg/kg tBuPrOcEst-BZT. Liver and/or kidney weights significantly increased ($p<0.05$) at doses ≥300 mg/kg, or 1000 mg/kg, respectively, for animals exposed to P-BZT, drometrizole, tBu-BZT, ditPe-BZT, tBuPrOcEst-BZT, bumetrizole, and diBu-ClBZT. Animals exposed to 1000 mg/kg tBuPrOcEst-BZT also had significant weight changes in several other organs. Animals with greater organ weight changes had greater changes in liver and kidney gene expression. These changes correspond to preliminary (and ongoing) pathology results which show lesions in the liver and kidney. In summary, Octrizole and diMeEtPh-BZT did not induce any test-article related changes in any of the endpoints observed. The seven other PBZTs evaluated showed changes indicative of kidney or liver toxicity, with tBuPrOcEst-BZT (the only PBZT containing an ester), displaying the most toxicity.

Poster Presentation 14

Exposure to an environmentally relevant oxidizer, potassium bromate, produces novel metabolic and mutational signatures that are distinct from the signatures of other redox stress agents

Degtyareva NP, Placentra VC, Klimczak LJ, Gabel SA, Mueller GA, Smirnova TI, and Doetsch PW
Mutagenesis and DNA Repair Regulation Group, DIR GISBL, NIEHS, Integrative Bioinformatics Support Group, NIEHS, Nuclear Magnetic Resonance Research Core Facility, NIEHS, Department of Chemistry, North

Potassium bromate is an environmentally relevant oxidizing agent that is added to flour during bread making in the United States and is used in hair care products. The use of potassium bromate has been banned in Europe, Canada, and Asia due to concern for potential health effects including cancer, reproductive damage, and other deleterious effects. Exposure of rodents to potassium bromate causes an increase in the incidence of cancers, and mutation frequencies. We report here deciphering the mutational signature of potassium bromate in yeast single strand DNA. Defining this signature revealed the heterogeneity of the mutational signatures of several redox stress agents. To understand the molecular mechanisms underlying the differences in mutational signatures of potassium bromate, hydrogen peroxide and paraquat, we utilized proton nuclear magnetic resonance and analyzed alterations in metabolic landscapes following exposure to these agents. Although hydrogen peroxide and potassium bromate are often referred to as “generic” oxidative agents and are interchangeably used in the studies addressing contribution of redox stress to disease and aging, we observed distinct and profoundly different metabolic signatures caused by potassium bromate and hydrogen peroxide. In addition, we uncovered paradoxical (and unique to potassium bromate) augmentation of its mutagenicity and cytotoxicity by thiol-containing antioxidants. By employing spin trap electron paramagnetic resonance spectroscopy, we detected an uncommon, short-lived reactive species generated by interaction of potassium bromate with these antioxidants *in vitro*. Our study provides the framework for understanding multidimensional processes triggered by exposure to agents collectively known as oxidants and may be clinically relevant as biomarkers of different types of redox stress.

Poster Presentation 15

Glucocorticoids suppress NLRP3 Inflammasome activation through transcriptional metabolic reprogramming of the IRG-1 in macrophages

Diaz-Jimenez DO, and Cidlowski JA
Molecular Endocrinology, DIR STL, NIEHS,

Synthetic glucocorticoids are one of the most prescribed anti-inflammatory and immunomodulatory agents. The action of the glucocorticoids in immune cells are mediated by the glucocorticoid receptor (GR) acting as a ligand-dependent transcription factor. Emerging evidence also shows the involvement of macrophages in the pathogenesis of several inflammatory diseases, including atherosclerosis, type 2 diabetes (T2D) and obesity. Activation of macrophages in response to pathogens and tissue damage induces transcriptional metabolic reprogramming to resolve the inflammation and restore the homeostasis. We hypothesize that glucocorticoids contribute to macrophages activation and polarization and shape the inflammatory response through regulation of genes associated with metabolism. Using primary bone marrow-derived macrophages (BMDM) from the specific myeloid-GR knockout mice (myeGRKO) we demonstrate that GR-deficient macrophages become hypersensitive to *in vitro* LPS-induced inflammation and display increased expression of pro-inflammatory molecules such as IL1B and TNF. Metabolomic approaches (mass spectrometry and seahorse experiments) show that GR-deficient macrophages display differential dependence on metabolic pathways for energy production including altered mitochondrial metabolism, tricarboxylic acid (TCA) cycle metabolism and glycolytic activity. Interestingly, pro-inflammatory GR-deficient macrophages fail to downregulate the expression of the enzyme IRG-1/ACOD1 that catalyzes the aconitate-to-itaconate reaction resulting in higher levels of itaconate and succinate, two of the TCA cycle metabolites that link metabolism and innate immunity. Finally, we provide compelling data showing that glucocorticoids prevent the NLRP3 inflammasome activation of macrophages by regulating the expression of IRG-1 and the levels of itaconate. Our results reveal that the glucocorticoid receptor enhance responses to inflammation connecting mitochondria metabolism, oxidative stress responses and immune response. Conversely, the loss of glucocorticoid signaling in macrophages promotes a pro-inflammatory metabolic reprogramming associated with the lack of regulation of IRG-1, mitochondrial dysfunction and accumulation of TCA metabolites, all of which are implicated directly in NLRP3-inflammasome activation.

Poster Presentation 16

Utilization of Soluble Cre for Gene Editing in Mouse Endometrial Epithelial Organoids.

Dickson MJ, Ray M, and DeMayo FJ
Pregnancy & Female Reproduction, DIR RDBL, NIEHS, Pregnancy & Female Reproduction, DIR RDBL, NIEHS,

The endometrium is the innermost layer of the uterus and is comprised of epithelial and stromal cells. Cross-communication between the two cell types is critical for endometrial function and normal fertility. Conditional uterine knock-out mouse models are commonly used to determine the role of specific genes in endometrial function. While these models are valuable, they are also slow and laborious, and can make it difficult to determine the impact of a specific gene deletion in the stromal cells or epithelial cells alone. *In vitro* culture methods allow for more in-depth analysis on a specific cell type. More recently, investigators have developed endometrial epithelial organoids to better understand cellular mechanisms in endometrial epithelial cells. Endometrial epithelial organoids are created from uteri and grown in solubilized basement membrane matrix (Matrigel) to allow for three-dimensional growth. The ability to genetically manipulate endometrial epithelial organoids in vitro could uncover mechanisms for specific genes in endometrial epithelial cells. The use of organoids could help explain the role of epithelial cells in phenotypes observed in conditional uterine gene ablation in mice. Our objective was to develop organoids from reporter mice to validate the technique and employ a soluble Cre recombinase to genetically modify organoids. Specifically, we used *R26-CAG-LSL-Sun1-sfGFP-Myc* (Jax 021039) mice which have floxed STOP cassette so when Cre is active, the cells express a SUN1-GFP fusion protein in the nuclear membrane. To develop organoids, uteri were dissected from five-day old pups and uteri were chopped into 2-4 mm pieces then enzymatically digested with 1% Trypsin solution for 90 minutes at 4°C. Following digestion, cells were cultured in Matrigel droplets and in the presence of medium containing growth factors to allow for organoid development. Once organoids developed and were grown to confluency, they were passaged. During the passaging process, organoids were incubated in the absence or presence of 8 µM TAT-Cre produced in *E. coli* (Millipore sigma SCR508) in medium for four hours at 37°C to remove the STOP cassette. After the four-hour incubation, the organoids were washed and plated in Matrigel droplets in the presence of growth medium. Following five days of growth post-incubation with soluble TAT-Cre, organoids were evaluated for STOP cassette excision and GFP expression. Organoids that were incubated with soluble TAT-Cre successfully had the STOP cassette excised, expressed SUN1-GFP fusion protein, and were fluorescent. This confirmation of Cre recombinase activity in the organoid system opens the door for future genetic manipulation studies in endometrial epithelial organoids. Employing soluble TAT-Cre on endometrial epithelial organoids will allow investigators to study mechanisms in epithelial cells that align with phenotypes seen from uterine genetic alterations in the mouse.

Poster Presentation 17

Lipid Metabolism in Neural Differentiation of Embryonic Stem Cells

Fan W, and Xiaoling L
Metabolism, Genes, and Environment, DIR STL, NIEHS,

Central nervous system is enriched with several types of lipids that are important for maintaining normal physiological functions of the neurons and structural development of the brain. Dysregulation of homeostasis of these lipids, including sphingolipids and very long-chain fatty acids, has been associated with numerous human neurological diseases, such as neurodegenerative diseases and neurodevelopmental disorders.

We recently showed that degradation of sphingolipids is under transcriptional control of SIRT1, a highly conserved mammalian NAD+-dependent protein deacetylase, in mouse embryonic stem cells (mESCs). Deletion of SIRT1 results in accumulation of sphingomyelin, the most abundant mammalian sphingolipid, in mESCs, primarily due to reduction of SMPDL3B, a GPI-anchored plasma membrane bound sphingomyelin phosphodiesterase. Mechanistically, SIRT1 is highly expressed in mESCs cells, where it functions to promote c-Myc-mediated transcription of *Smpdl3b* gene and subsequent sphingomyelin degradation. Functionally, SIRT1 deficiency-induced accumulation of sphingomyelin increases membrane fluidity of mESCs and impairs their neural differentiation in vitro and in vivo. Additionally, we found that defects in lipid metabolism in peroxisomes, cellular organelles important for a variety of metabolic processes, including antioxidant defense, β-oxidation of very-long-chain fatty acids, and membrane lipids synthesis, also impair neural differentiation of mESCs. Deletion of Pex5 or Pex19, two protein factors mediating peroxisome membrane biogenesis and matrix enzyme import, disturbs normal peroxisomal functions in lipid metabolism. In consequence, the normal neural differentiation process of those cells is significantly disturbed.

Our findings uncover new molecular mechanisms regulating lipid homeostasis in mESCs, and highlight the importance of lipid metabolism in neural differentiation of embryonic stem cells.

Poster Presentation 18

The Mosquito Protein AEG12 as a Scaffold for Novel Antiviral Therapeutics

Foo AC, Chen S, Martin N, and Mueller GA
Nuclear Magnetic Resonance, DIR GISBL, NIEHS, Neurobiology Laboratory,

The mosquito protein AEG12 consists of 12 amphipathic alpha-helices enclosing a large central cavity which can bind a range of hydrophobic ligands, with a mixture of saturated and unsaturated fatty acids representing its natural substrates. AEG12 is noticeably upregulated in response to viral infection, suggesting that this protein and its associated lipid cargoes may have antiviral properties. Indeed, previous work in our group showed that AEG12-mediated delivery of these naturally-occurring fatty-acid ligands destabilizes the protective lipid bilayer of enveloped viruses, giving rise to robust antiviral activity with micromolar IC50's against a range of pathogens such as Zika virus, lentivirus, and human coronaviruses including COVID-19, albeit at the cost of significant cytotoxic activity. The large cavity of AEG12 can also bind a range of exogenous ligands including plant phenolics and pesticides, raising the possibility that AEG12 could be used as a delivery vehicle for hydrophobic, non-natural viral inhibitors such as lysophosphocholine (LPC) and ginkgolic acid (GA); both of which have been shown to inhibit viral membrane fusion, reducing infectivity independent of membrane destabilization and its associated cytotoxic effects. Alternatively, the lipophilic nature of AEG12 could allow it to mediate the reverse reaction; extracting lipids from the viral envelope to provide a secondary ligand-independent mechanism of antiviral activity that could be used to expand the therapeutic profile of AEG12. In this work, we demonstrate that AEG12 can be successfully loaded with both LPC and GA. AEG12-mediated delivery of the latter into model bilayer systems significantly reduced the rate of membrane fusion, resulting in robust antiviral activity while minimizing membrane perturbation. In a separate course of study, we demonstrate that the Apo-form of AEG12 is able to effectively extract lipids from model membranes, with on/off kinetics on the minute timescale. This rapid exchange process induces transient perturbations and vesicle leakage in model membranes, though its impact on mammalian cell viability is negligible on account of their large size and active membrane-repair pathways. However, the small size and lack of lipid replenishment mechanisms increases the vulnerability of enveloped viruses to this disruption, resulting in modest inhibition of both Lentivirus and HIV. These studies provide two unique biophysical mechanisms through which the lipophilic and lipid-delivery properties of AEG12 can give rise to robust antiviral activity while minimizing its cytotoxic side effects, with implications for the design of novel therapeutic strategies.

Poster Presentation 19

Searching for U: Cryo-EM Structures of the SARS-CoV-2 Endoribonuclease Nsp15 Reveal Insight into Nuclease Specificity and Dynamics

Frazier MN, Dillard LB, Krahn JM, Perera L, Williams JG, Wilson IM, Stewart Z, Pillon MC, Deterding LJ, Borgnia MJ, and Stanley RE
Nucleolar Integrity, DIR STL, NIEHS, GISBL, ESCBL,

SARS2, a novel betacoronavirus, emerged early last year causing a global pandemic. Nsp15 is an endoribonuclease, encoded by the SARS2 viral genome that cleaves viral RNA 3' of uridines. It is primarily believed to cleave the polyU tail of the negative strand intermediate RNA in order to help the virus evade immune system detection. Studies in cell culture and animal models have shown that Nsp15 deficient coronaviruses lead to increased interferon responses and higher survival compared to WT viruses. Nsp15 is found in all coronaviruses, therefore it is a promising therapeutic target for SARS2, as well as other coronaviruses responsible for human respiratory illnesses (common cold, SARS1, MERS). The specificity and molecular mechanism of RNA processing by Nsp15 are poorly understood. Nsp15 must assemble into a hexamer to cleave RNA, therefore we hypothesized that the architecture of complex is critical for regulating nuclease activity. **Our goal was to determine structures of Nsp15 in pre- and post-cleavage states to better understand how it recognizes and cleaves RNA, ultimately providing insight into how it could be targeted.**

We determined the first series of cryo-EM reconstructions of SARS2 Nsp15, in apo, UTP-bound, and pre- and post- cleavage states, at resolutions ranging from 2.2 to 3.3Å. Our seven cryo-EM reconstructions, combined with biochemistry, mass spectrometry, and molecular dynamics, exposed molecular details of how critical active site residues recognize uridine and facilitate catalysis of the phosphodiester bond. A key serine residue forms hydrogen bonds with the uracil base, while a tyrosine in the active site forms van der waals interactions with the ribose. The RNA bound structures suggested that two conserved histidine residues support RNA cleavage through a transesterification reaction. This mechanism was confirmed by mass spectrometry, which revealed the accumulation of the cyclic phosphate transesterification product. Gel-based and FRET cleavage assays revealed additional sequence preferences beyond the uridine, specifically a preference for a purine in the position after uridine. Analysis of the apo and UTP-bound datasets revealed conformational dynamics that are likely important for substrate recognition and nuclease activity. Collectively, these findings advance our understanding of how Nsp15 processes viral RNA and provide a structural framework for the development of new therapeutics.

Poster Presentation 20

Mutations in the essential gene spoT confer resistance to ciprofloxacin in the microbial pathogen Pseudomonas aeruginosa

Garcia Villada L, Brooks AM, Degtyareva NP, and Doetsch PW
Mutagenesis and DNA Repair Regulation Group, DIR GISBL, NIEHS, Integrative Bioinformatics Support Group, NIEHS,

During our studies designed to establish an appropriate system to determine whether mutagenesis at the level of transcription (transcriptional mutagenesis) plays a role in the acquisition of antibiotic resistance in microbial pathogens, we found that most *Pseudomonas aeruginosa* antibiotic-resistant mutants scored on selective ciprofloxacin plates, carry mutations in genes involved in the regulation of the Stringent Response (SR), a bacterial stress response in reaction to amino-acid starvation, fatty acid limitation, iron limitation, heat shock, and other stress conditions. Among these, *spoT* (one of the major components of the SR) mutations were found in about 40% of ciprofloxacin-resistant isolates. We also found that 75% of the mutations were insertions/deletions (InDels), with short deletions as the most frequently occurring mutation type (almost 70% of all InDels). These results were completely unexpected, as many studies demonstrate that, in *P. aeruginosa*, ciprofloxacin resistance is mostly acquired through base substitutions in *gyrA* or in repressor genes of different efflux pumps. In addition, *spoT* is an essential gene for many bacteria, including P. *aeruginosa*, and reported mutations in this gene that are compatible with viability are quite rare. The partial or total inactivation of *spoT* is expected to upregulate the SR. Through a series of preliminary experiments, we have now determined that most of the observed mutations are induced on the selective plates in a subpopulation of cells that are not immediately killed by ciprofloxacin. In conventional studies, these mutations are usually not noticed because they induce slow growth and resistant mutants are scored on the plates before the carriers of these mutations can form a colony. In our studies, we grew the cells in minimal media supplemented with 0.25% sodium citrate before plating; under these conditions, most of the cells reach stationary phase carrying only one copy of the chromosome and, thus, induced mutations are expressed earlier, i.e., phenotypic lag is diminished. Our results suggest that the SR may be an important factor during the acquisition of microbial antibiotic resistance.

Poster Presentation 21

Neighborhood Deprivation and Sleep Health in a Racially/Ethnic Diverse Cohort of U.S. Women

Gaston Harrison SA, Lawrence KG, Sandler DP, and Jackson CL
Social & Environmental Determinants of Health Equity Group, DIR EB, NIEHS, Chronic Disease Epidemiology Group, DIR EB, NIEHS,

Introduction: Although neighborhood environments have been shown to affect sleep health, few studies have directly measured multiple indicators of both neighborhood deprivation and sleep while considering modification by race/ethnicity.

Methods: Among 49,833 eligible U.S. women enrolled in the Sister Study from 2003 to 2009, we investigated associations between neighborhood deprivation (e.g., percentage of residents unemployed, household crowding) and multiple sleep dimensions. Participants' addresses were linked to U.S. census block group level Area Deprivation Index rankings (range: 1-100) for the year 2000, and participant rankings were divided into quintiles where the highest quintile represented the highest deprivation level. Participants self-reported habitual sleep duration, sleep debt, frequent napping, and insomnia symptoms. Adjusting for sociodemographic and clinical characteristics, we used Poisson regression with robust variance to estimate prevalence ratios (PRs) and 95% confidence intervals (CIs) for sleep dimensions among participants within quintiles (Qs) 2-5 vs. Q1. Interaction terms were used to assess modification by race/ethnicity.

Results: Mean age ± standard deviation was 55 ± 9 years. Women with higher neighborhood deprivation were more likely to self-identify as a racial/ethnic minority and had higher unadjusted prevalence of poor sleep dimensions. After adjustment, higher ADI was associated with very short sleep (≤5 hours), and race/ethnicity was a modifier (e.g., race-stratified results for Q5 vs. Q1:PRWhite=1.31 [95% CI: 1.14-1.51], PRBlack=0.91 [0.71-1.18], PRHispanic/Latina= 1.17 [0.68-2.04], p-interaction <0.05). Although race/ethnicity did not modify remaining associations, women with higher neighborhood deprivation also had a higher prevalence of sleep debt, frequent napping, and insomnia symptoms. When compared to White women with the lowest neighborhood deprivation, Black women across all deprivation levels and Hispanic/Latina women in Q2-Q5 were substantially more likely to report each poor sleep dimension (PR range: 1.21 to 5.01).

Conclusion: A multidimensional measure of neighborhood deprivation was associated with poor sleep and sleep disparities among a diverse cohort of U.S. women.

Poster Presentation 22

Early-life exposures and age at breast development: Implications for breast cancer risk

Goldberg M, D'Aloisio AA, O'Brien KM, Zhao S, and Sandler DP
Chronic Disease Epidemiology, DIR EB, NIEHS, Social & Scientific Systems, DIR BCBB, NIEHS,

Early age at breast development (thelarche) has been associated with increased breast cancer risk. While average age at thelarche has declined over time, few risk factors for early thelarche apart from overweight status in childhood have been identified. We used a large, nationwide cohort of women born between 1928 and 1974 to assess the relationships between pre- and postnatal exposures and the timing of thelarche. Breast cancer-free women ages 35-74 years who had a sister diagnosed with breast cancer were enrolled in the Sister Study from 2003-2009 (N=50,884). At enrollment, participants reported their age at thelarche, which we categorized as early (≤10 years), average (11-13 years), and late (≥14 years), as well as information on early-life exposures. We estimated odds ratios (ORs) and 95% confidence intervals (CIs) for early and late thelarche relative to average age at thelarche using polytomous logistic regression for each early-life exposure, adjusted for birth cohort, race/ethnicity, and family income level in childhood. We examined modification by birth cohort, race/ethnicity, family income, relative weight at age 10, and extent of breast cancer family history through stratification. Early thelarche was more common in recent birth cohorts and among non-Hispanic Black and Hispanic women. Early thelarche (≤10 years) was associated with multiple prenatal exposures: maternal gestational hypertensive disorder (OR=1.25, 95% CI 1.09-1.43), maternal diethylstilbestrol (DES) use (OR=1.23, 95% CI 1.04-1.45), maternal smoking during pregnancy (OR=1.20, 95% CI 1.13-1.27), and young maternal age (OR 1.30, 95% CI 1.16-1.47 for <20 vs 25-29 years). Being firstborn was also associated with early thelarche (OR=1.25, 95% CI 1.17-1.33). Low birthweight (<2500 vs 2500-3999g) was suggestively associated with both early (OR=1.06, 95% CI 0.96-1.17) and late (OR=1.15, 95% CI 1.05-1.25) thelarche, as was use of soy formula in infancy (Early: OR=1.10, 95% CI 0.93-1.30; Late: OR=1.07, 95% CI 0.92-1.25). Patterns were generally similar across strata of modifiers of interest. The associations we observed between pre- and postnatal exposures and age at thelarche suggest that the early-life environment influences breast development and therefore may also affect breast cancer risk by altering the timing of pubertal breast development.

Poster Presentation 23

Structure of the multi-functional human scaffolding protein PELP1 bound to WDR18 reveals insight into its diverse cellular functions.

Gordon J, Viverette E, Borgnia MJ, and Stanley RE
Nucleolar Integrity, DIR STL, NIEHS, Molecular Microscopy Consortium, DIR GISBL, NIEHS,

Scaffolding proteins are crucial regulators of many cellular signaling and metabolic pathways. PELP1 (Proline, Glutamate and Leucine Rich Protein 1) is an essential human nuclear receptor coregulator with a multitude of genomic and nongenomic functions, including steroid hormone-based transcriptional regulation and large ribosomal subunit (60S) synthesis. In the nucleus, PELP1 is widely implicated in 17b-estradiol (E2) signaling by acting as an estrogen receptor (ER)-interacting protein that influences downstream gene expression. In the nucleolus, PELP1 is required for proper pre-ribosomal RNA (pre-rRNA) processing of the 60S subunit. PELP1 is a component of a conserved protein assembly known as the Rix1 complex (PELP1-WDR18-TEX10-SENP3) largely known for its role in 60S synthesis but scarcely studied in nuclear receptor signaling. Importantly, PELP1 expression and deregulation in humans has been identified as a driver in a variety of hormonal cancers including breast, endometrial, ovarian and prostate cancer. This underscores the importance of studying PELP1 and its molecular context within the Rix1 complex (WDR18, TEX10, SENP3). In this study, we have asked how does PELP1 assemble into the larger human Rix1 complex and how does this protein complex act as a regulatory scaffold? Using mammalian cells, we expressed and purified the recombinant Rix1 complex and determined the molecular requirements for complex assembly. We identified that the highly conserved N-terminal region of PELP1 and wild-type WDR18 can form a stable core called the Rix1 sub-complex (Rix1 SC). We further purified the Rix1 SC in isolation and used Cryo Electron Microscopy for high-resolution structure determination. We solved the structure of the human PELP1-WDR18 sub-complex to 3.6 A resolution and revealed that this sub-complex forms a heterotetrameric (dimer of dimers) assembly. This resolution allowed for visualization of PELP1’s many nuclear receptor interacting motifs (LXXLL) that facilitate steroid receptor binding, as well as the localization of these motifs within the overall sub-complex assembly. This study for the first time has established the high-resolution structural architecture of a critical protein and known proto-oncogene PELP1. Additionally, this study revealed that PELP1 forms a stable and higher-ordered sub-complex with WDR18. Future experiments will be directed at understanding the purpose of this sub-complex assembly and if it plays biological roles in the many known scaffolding/signaling duties of PELP1.

Poster Presentation 24

Identification of refinements in a murine model of lipopolysaccharide systemic inflammation in C57BL/6 mice

Goulding DR, Wiltshire RA, Shi M, and Blankenship-Paris TL
Veterinary Medicine Section, CMB, DIR, NIEHS, Comparative Medicine Branch, DIR, NIEHS, Biostatistics & Computational Biology Branch, DIR, NIEHS,

The aim of this study was to identify an optimal monitoring schedule and a more humane experimental endpoint than moribundity for the commonly used murine model of systemic inflammation created by lipopolysaccharide (LPS) administration. We developed a scoring sheet for behavioral and physical changes following IP injection of LPS that included: hunched posture, reduced activity, and reduced response to stimuli. Body temperatures and body weights were also recorded. Male (n=10) and female (n=10) C57BL/6 mice were subcutaneously implanted with temperature transponders for remote measurement of body temperature prior to injection with LPS. Animals were socially housed in static caging and provided with twice the standard amount of nesting material. Mice were injected intraperitoneally with either 5 mg/kg (n=10) or 10 mg/kg (n=10) LPS. Mice were monitored every two hours for 48 hours following injection with LPS and scored for each parameter. Moribundity was considered the clinical endpoint. At 48 hours, any remaining mice were euthanized. We observed moderate to high degrees of correlation between low body temperature and high clinical scores in the 5mg/kg male (Pearson correlation coefficient r=-0.42), 10 mg/kg male (r=-0.76), 5 mg/kg female (r=-0.67), and 10 mg/kg female (r=-0.73) groups. Results showed that mice with temperatures less than 25°C did not recover to normothermia and reached moribundity. We found the most critical times for observations (lowest body temperature and highest clinical sign scores) were 14-26 hours post injection. Based on these findings, we now recommend a combination of refinements to our investigators that include: monitoring every 2 hours beginning at 12 hours post injection, removal of animals with body temperatures less than 25°C, providing supplemental wet food (mash), and group housing in static caging with extra nesting material for thermoregulation.

Poster Presentation 25

Neighborhood Social Cohesion and Serious Psychological Distress among Asian, Black, Hispanic/Latinx, and White Men and Women in the United States

Gullett LR, Alhasan DM, Jackson II B, Gaston SA, Kawachi I, and Jackson CL
Social & Environmental Determinants of Health Equity Group, DIR EB, NIEHS, Social & Scientific Systems, Inc., a DHL holdings company, Department of Social and Behavioral Sciences, Harvard T.H. Cha

Serious psychological distress (SPD) is more common among women, older adults, and individuals with a low income. Prior studies have highlighted the role of low neighborhood social cohesion (nSC) in potentially contributing to SPD; however, few have investigated this association in a large, nationally representative sample of the United States. We used 2013-2018 data from the National Health Interview Survey to investigate nSC and SPD among Asian, Non-Hispanic (NH)-Black, Hispanic/Latinx, and NH-White men and women in the United States (N=168,573) and to determine modification by age and annual household income across race/ethnicity. nSC was measured by asking participants four questions related to the trustworthiness and dependability of their neighbors, and scores were trichotomized into low (<12), medium (12-14), and high (15-16). SPD was measured using the Kessler 6 psychological distress scale with scores ≥13 indicating SPD. After adjusting for sociodemographic, health behavior, and clinical confounders, we used Poisson regression with robust variance to estimate prevalence ratios (PRs) and 95% confidence intervals (CIs). The mean age ± standard error was 47±0.1 years, 51.9% were women, 68.9% were NH-White, and 58.9% of participants had household incomes <$75,000. Overall, low vs. high nSC was associated with a 75% higher prevalence of SPD (PR=1.75 [95% CI: 1.59-1.92]). Associations between low vs. high nSC and SPD varied by age (PR≥50 years old=1.92 [95% CI: 1.70-2.18]; PR<50 years old=1.58 [95% CI: 1.37-1.81]). The association between low vs. high nSC and SPD was greater among those with incomes ≥$75,000 vs. <$75,000 in Hispanics/Latinxs (PR≥$75,000=2.97 [95% CI: 1.45-6.08]; PR<$75,000=1.51 [95% CI: 1.16-1.98]). The inverse nSC-SPD relationship varied by age and income across race/ethnicity. Enhancing cohesion through trust and social support may help address SPD.

Poster Presentation 26

Characterization of reproductive and hormonal defects in mutant NuRD complex members, CHD4 and MTA3, in mouse model systems.

Headley KM, Chrysovergis K, and Wade P
Eukaryotic Transcriptional Regulation, DIR ESCBL, NIEHS,

The Mi-2/nucleosome remodeling and deacetylation (NuRD) complex is a highly conserved chromatin remodeling complex made of six core subunits. Functional members, CHD3/4/5, HDAC1/2, and MBD2/3 have unique functions guiding chromatin assembly, histone deacetylation, and DNA-binding respectively. The other members, MTA1/2/3, GATAD2A/B, and RBBP4/7 are believed to target, modulate, and/or structurally support NuRD complex activity. Recent studies have suggested that mutational perturbations to MTA3 and CHD4 have defects relating to hormone regulation and reproduction. The current study explores previously uncharacterized phenotypes displayed by MTA3 and CHD4 mutants using murine model systems.

Poster Presentation 27

Signature motif of glycidamide-induced hypermutation in single-stranded DNA is ubiquitous in human cancers

Hudson K, Klimczak LJ, Sterling JF, Burkholder AB, Saini N, Mieczkowski P, and Gordenin DA
Mechanisms of Genome Dynamics, DIR GISBL, NIEHS, Integrative Bioinformatics Support Group, NIEHS, Department of Biochemistry & Molecular Biology, Medical University of South Carolina, Charleston, SC,

Acrylamide is a probable human carcinogen and naturally occurs in many commonly consumed processed foods and tobacco smoke. Once ingested, acrylamide can be converted to the more mutagenic epoxide glycidamide through a cytochrome P450 enzyme. Previous studies by others have characterized glycidamide-induced mutagenesis; however, their experimental systems could not explicitly identify which bases form mutagenic lesions *in vivo*. To address this, we utilized yeast strains with a temperature-sensitive mutation that causes telomere uncapping and 5' to 3' end resection at non-permissive temperatures, leading to transient multi-kilobase stretches of subtelomeric single-stranded DNA (ssDNA) and facilitating unambiguous identification of bases forming mutagenic lesions. Glycidamide exposure induced hypermutation preferentially in ssDNA, and mutagenesis required functional translesion synthesis (TLS). Whole genome sequencing indicated the mutagenic ssDNA lesions were predominantly formed in C and A, suggesting a novel mechanism for glycidamide mutagenesis. C->G and A->G were the predominant mutations and were dependent on the TLS polymerase Rev1, consistent with its dCTP terminal transferase activity. Motif analyses identified a significant preference for mutagenic lesions to occur in central As in 5'-n**A**t-3' trinucleotides, suggesting a n**A**t->n**G**t as a signature mutational motif of glycidamide in ssDNA. We found a significant enrichment of this mutational motif and a lesser n**A**t->n**T**t motif across human cancers, and found a significant correlation between n**A**t->n**G**t mutagenesis and tobacco smoking, a known source of acrylamide exposure. Future work includes quantifying the extent of glycidamide lesion formation and repair in dsDNA, determining if glycidamide's mutational motif is shared by other mutagenic molecules with similar chemistry, and exploring alternative TLS pathway choices that might be contributing to the lesser presence of the n**A**t->n**T**t motif. Identifying mechanisms that contribute to glycidamide-induced genomic instability can provide valuable knowledge that may guide public policy and ultimately prevent and/or cure cancer.

Poster Presentation 28

ZATT (ZNF451) is a novel nuclear RNA/DNA hybrid cleaving enzyme

Jaguva Vasudevan A, Riccio A, Appel C, and R. Scott W
Structural Cell Biology group, NIEHS,

ZATT (ZNF451) is a multifunctional nuclear protein participating in the repair of Topoisomerase 2 mediated DNA damage, DNA replication, and transcription. These nuclear activities all have been linked to ZATTs intrinsic amino terminal E3 SUMO2/3 ligase activity. At the protein level, ZATT also contains an array of central C2H2 class Zinc finger motifs, and a carboxyl-terminal PIN/NYN family nuclease domain of unknown function (DUF). Here we report that in addition to its SUMO ligase activity, recombinant purified ZATT harbors intrinsic ribonuclease activity. The broad Mg2+ and Mn2+ dependent ZATT nuclease activity displays a preference for RNA/DNA > ssRNA > dsRNA, but fails to cleave ssDNA or dsDNA containing substrates *in vitro*. In the context of RNA/DNA hybrids, ZATT displays an RNASEH1-like activity, and efficiently cleaves embedded ribonucleotide containing substrates with stretches of 5 or more ribonucleotides. Using a deletion approach, we generated fragments of ZATT containing its PIN domain and flanking Zinc-finger motifs and analyzed activity on model RNA/DNA hybrid substrates. This approach mapped the minimal maximally active nucleolytic core to encompass 2 flanking Zn-fingers and the PIN domain. The PIN core also cleaves RNA/DNA hybrids in isolation, but its activity was 10-fold less active than the Znf-PIN fragments. To define the basis for ZATT catalytic activity, we determined a 2.3 Angstrom resolution structure of ZATT-PIN that unveils an extensive dimeric interface. ZATT exists as a stable dimer in solution as assessed by Multi angle laser light scattering (MALS), and mutation of the ZATT dimerization interface abrogates activity. Previous protein-protein interaction studies in the lab have mapped a Topoisomerase 2 binding region of ZATT to its nuclease core. Intriguingly, the addition of purified Top2 to ZATT nuclease reactions suppresses ZATT RNA/DNA hybrid cleavage, and Top2 binding triggers an array of conformational changes that block ZATT active site access. These data highlight an intricate mode of allosteric regulation of ZATT activity by Top2. Consistent with a role for ZATT in processing cellular RNA/DNA hybrids, we find that ZATT co-immunoprecipitates with the RNA/DNA hybrid-specific anti-S9.6 antibody. Together, results from biochemical and structural analysis point to possible roles for ZATT in the nucleolytic regulation of RNA/DNA hybrids. Future work aims to identify cellular targets of the ZATT ribonuclease.

Poster Presentation 29

Dysregulation of NTHL1 causes sensitivity to cisplatin in human cells

Kar A, Degtyareva N, and Doetsch PW
Mutagenesis and DNA Repair Regulation Group, DIR GISBL, NIEHS,

Base excision repair (BER) plays a critical role in the maintenance of genome stability by repairing potentially mutagenic DNA base damages and preventing events leading to tumor development. NTHL1, a bifunctional DNA glycosylase initiates the BER pathway primarily through recognition and removal of oxidized pyrimidines. Loss of NTHL1 expression or function has been linked to several human cancers. However, our recent analysis across different databases shows that in several cancers NTHL1 exhibits mRNA over-expression. Recent work from our group established that transient over-expression of NTHL1 leads to acquisition of several hallmarks of cancer in non-tumorigenic immortalized cells likely through interaction with the nucleotide excision repair (NER) protein XPG.

Here, we investigate how NTHL1 expression levels in five (H522, H226, A549, H1792, H1975) non-small cell lung carcinoma (NSCLC) cell lines affect their sensitivity to cisplatin, a widely used anticancer drug that induces several types of DNA adducts including intra- and interstrand crosslinks that are primarily repaired by NER. We chose NSCLC cell lines with different NTHL1 expression levels and tested their sensitivities to cisplatin. We report here that the cell line with lowest expression of NTHL1 (H522) shows the highest resistance to cisplatin indicating that decrease in NTHL1 levels may modulate resistance to crosslinking agents in NSCLC tumors. In a complementation study, overexpression of NTHL1 in H522 cell line sensitized it to cisplatin. These experiments reveal a previously unknown link between NTHL1 expression levels and cisplatin sensitivity of NSCLC tumor cells. Our study may provide insight into predicting cisplatin sensitivity in NSCLC.

Poster Presentation 30

Communication network within Rix7 AAA-ATPase to drive ribosome assembly

Kocaman S, Kocaman S, Lo Y, Krahn JM, Sobhany M, Dandey VP, Petrovich M, Williams JG, Deterding LJ, Borgnia MJ, and Stanley RR
Nucleolar Integrity, DIR STL, NIEHS, Genome Integrity and Structural Biology Laboratory, NIEHS, Epigenetics and Stem Cell Biology Laboratory, NIEHS,

Rix7 is an essential AAA-ATPase that functions during the early stages of ribosome biogenesis and has been linked to cancer and neurodegenerative diseases. Rix7 is composed of three domains including an N-terminal domain and two AAA+ domains known as the D1 and D2 domains that assemble into an asymmetric hexamer. We previously established that Rix7 is a molecular unfoldase that translocates substrates through its central pore, however the regulation of substrate unfolding and how the different Rix7 domains coordinate their activities within the overall hexameric structure was unknown. By capturing cryo-EM structures of Rix7 in different ATP bound states we observed that loss of nucleotide binding in the D1 domain triggers rigid body conformational changes that drive the rearrangement of individual Rix7 protomers during the processive cycle of substrate translocation. The disordered NTD was not visible in any of our cryo-EM reconstructions, signifying that it is flexible and dynamic. Cross-linking mass spectrometry revealed that the NTD translocates through the central channel, suggesting a role for the NTD in regulating substrate access to the central channel. Deletion of the disordered NTD enabled us to obtain a structure of the Rix7 hexamer to 2.9 Å resolution, providing high resolution details of critical motifs involved in substrate translocation and inter-domain communication. This structure coupled with cell-based assays established that the linker connecting the D1 and D2 domains as well as the pore loops lining the central channel are essential for formation of the large ribosomal subunit. Together, our work shows that Rix7 utilizes a complex communication network within its hexameric structure to drive ribosome biogenesis.

Poster Presentation 31

RNA editing by APOBEC3 cytidine deaminases

Kockler ZW, Klimczak LJ, Bostan H, Li J, Roberts SA, and Gordenin DA
Mechanisms of Genome Dynamics, DIR GISBL, NIEHS, Bioinformatics Support Group, NIEHS, NC, School of Molecular Biosciences, Washington State University, Pullman, WA,

APOBEC3A (A3A) and APOBEC3B (A3B) cytidine deaminases cause hypermutation in single-stranded (ss) DNA by converting cytosines into uracils, which following DNA replication are fixed into thymines. The cytosine deamination predominantly occurs in a tCn trinucleotide motif (with significant preference to tCa) providing a distinguishing feature for A3A and A3B-induced ssDNA hypermutation in model systems as well as in cancer genomes. However, recent studies revealed that cytidine deamination by APOBEC3 family members occurs not only in ssDNA, but also in mRNAs (editing) and RNA virus genomes (hypermutation). Further, the reported hypermutated viral genomes contain an abundance of uCn trinucleotide motifs (analogous to tCn in DNA) suggesting that A3A and/or A3B may be responsible, and such hypermutation could greatly affect the evolution and population dynamics of these RNA viruses. Here, we present the experimental and analytical designs for defining the RNA editing signature motifs of A3A and A3B. We analyzed previously published human mRNA and rubella virus genome RNA editing data as well as the APOBEC-induced DNA mutations in yeast. We calculated the enrichment and P-values for each of the 16 possible trinucleotide motifs containing C to U (RNA) and C to T (DNA) substitutions. We found that tCa is the most enriched A3A induced mutational motif for ssDNA, consistent with (Chan et al, 2015). However, when the same approach was used for previously published mRNA editing datasets, that have an increase in A3A expression, or hypermutated rubella RNA genomes, we found that tCg is significantly more enriched as compared to tCa. Additionally, we utilized yeast overexpressing either A3A or A3B to identify signatures specific to mRNA editing by each enzyme. We were successful in the detection of mRNA edits with A3A and A3B. We then found in A3A a statistically significant enrichment of tCn motifs. Of those enriched tCn motifs, the tCg editing motif was significantly more enriched than tCa, consistent with our analyses of mRNA editing in human cells and in rubella RNA genome. Together these results support the conclusion that A3A can edit mRNA, and unlike in ssDNA, tCg is the most preferred motif. This work will help identify the role APOBECs play in the editing of mRNA and may also help to understand the role of these enzymes in the evolution and population dynamics of RNA viruses.

Poster Presentation 32

Soy-based infant formula feeding and uterine fibroid incidence in a prospective ultrasound study of African American women

Langton CR, Harmon QE, Upson K, and Baird DD
Women's Health, DIR EB, NIEHS, Department of Epidemiology and Biostatistics, College of Human Medicine, Michigan State University,

Background: Uterine fibroids are highly prevalent, non-cancerous tumors of the myometrium and are the leading cause for hysterectomy in the United States. African American women are disproportionally burdened by fibroids and experience onset 5-10 years earlier than U.S. white women. Soy-based infant formula contains high concentrations of genistein, a phytoestrogen that can bind to estrogen receptors in mammals. Exposure during sensitive developmental windows may have detrimental effects on female reproductive systems. Laboratory studies of Eker rats and mice, respectively, have demonstrated that postnatal genistein exposure increased fibroid incidence in adulthood, and produced tissue alterations of posteriorization in the reproductive tract. No prior epidemiologic study has examined the association between soy formula feeding in infancy and prospectively assessed, ultrasound-detected incident fibroids in adulthood.

Methods: We evaluated this association among 1,581 African American women in the Study of Environment, Lifestyle & Fibroids (SELF). Participants were enrolled from 2010 to 2012 and were aged 23 to 35 years at baseline. Exposure to soy formula was assessed via an early life questionnaire administered to the participant's mother if she was available. To identify fibroid-free women at enrollment and assess fibroids during follow-up, a transvaginal ultrasound examination was conducted to detect fibroids ≥0.5 cm diameter during 4 clinic visits at approximately 20-month intervals. Self-reported health-related behaviors were also assessed at each visit. We used Cox proportional hazards models with age as the timescale to estimate hazard ratios (HRs) and 95% confidence intervals (CIs) for the association between soy formula feeding and incident fibroids adjusted for early life, reproductive, and lifestyle factors.

Results: Of 1,121 fibroid-free participants at baseline, 269 (24%) had incident fibroids detected during 4,841 person-years of follow-up. For 89% of participants, soy formula data were provided by the participant's mother. We did not observe an association between ever being fed soy formula as an infant and incident fibroid risk (HR 1.05, 95% CI: 0.74, 1.51). However, we did observe that participants fed soy formula within 2 months of birth and for 6 months or longer, compared to those never fed soy formula, had a 44% increased risk of fibroid incidence (HR 1.44, 95% CI: 0.86, 2.42). When we additionally adjusted for adult participant factors, the association was stronger in magnitude (HR 1.56; 95% CI, 0.92-2.65).

Conclusion: In the first study of soy formula feeding and prospectively assessed, ultrasound-detected incident fibroids, there was suggestive evidence that soy formula feeding in infancy, particularly soon after birth and for a longer duration, is associated with increased risk of fibroids.

Poster Presentation 33

TRIM28 regulates uterine function by modulating steroid receptor signaling

Li R, Wang T, Wu S, and DeMayo F
Pregnancy & Female Reproduction, DIR RDBL, NIEHS, Integrative Bioinformatics, NIEHS,

The ability of the uterus to support pregnancy is tightly regulated by the Progesterone Receptors (PGR) and Estrogen Receptors (ESRs) . Using Rapid Immunoprecipitation Mass spectrometry for PGR in human endometrial stromal cells (HESCs), Tripartite Motif Containing 28 (TRIM28) was identified as an interacting protein of PGR. TRIM28 is critical in maintaining the pluripotency of the stem cells and the specialized functions of multiple differentiated tissues However, its roles in uterus are still unknown. Therefore, we hypothesized that PGR is critical for the regulation of uterine function in mouse and humans.

By conducting knockdown (KD) TRIM28 in the primary HESCs, we found TRIM28 KD impaired the proliferation, migration and hormonal induced decidualization of HESCs. RNA-Seq analysis revealed that TRM28 KD already disrupted the transcriptome of in the pre-decidual cells which was the fundamental cause of the decidualization problems. ChIP-Seq revealed the genome wide binding of TRIM28. ATAC-Seq analysis indicated that TRIM28 KD increased the chromatin accessibility. Immunoprecipitation-mass spec further indicates that TRIM28 may directly interact with chromatin modifiers, transcription factors, metabolism enzymes etc. to regulate the HESC functions.

To determine the role of TRIM28 in vivo, TRIM28 was conditionally ablated in the mouse uterus using Pgr-cre (TRIM28d/d). TRIM28d/d mice were infertile due to the inability of the uterus to undergo a hormonal induced decidual response. The wildtype uterus mainly contained TRIM28+/ PGR+/ ESR1+ stromal cells, whereas the TRIM28d/d stroma consisted of TRIM28-/ PGRlow/ ESR1high cells and TRIM28+/ PGR-/ ESR1- cells. Crossing TRIM28d/d mouse with Sun1-GFP mice, we found the TRIM28-/ PGRlow/ ESR1high were derived from the PGR+ cells as expected, while TRIM28+/ PGR-/ ESR1- stromal cells were from PGR- cells. scRNA-Seq revealed the altered cell sub-population in the TRIM28d/d mouse uterus. All these results implied a potential role of TRIM28 in uterine remodeling.

The PGR induced Indian hedgehog, Ihh, was reduced in the uterine epithelium of TRIM28d/d mouse in spite of the normal epithelial levels of PGR suggesting suppressed epithelial PGR activity. In contrast, the expressions of stromal PGR were reduced in the TRIM28d/d uterus probably reduced stromal ESR1 signaling. Although the stromal ESR1 expressions was normal, ChIP-qPCR analysis indicated ESR1 binding at the *Pgr* promoter was decreased in the TRIM28d/d uterus. Therefore, it appears that TRIM28 regulates steroid hormone signaling in a uterine compartment specific manner. In summary, our study indicated that TRIM28 is a key regulator in uterine biology in both human and mice.

Poster Presentation 34

The Role of Serum Response Factor in Regulating Hormonal Responsiveness in the Uterine Function

Li W, Emery O, Wang T, Zhou L, Wu S, and DeMayo F
Pregnancy & Female Reproduction, DIR RDBL, NIEHS, Integrative Bioinformatics Support Group, NIEHS,

Proper functioning of progesterone signaling in the uterus is essential for successful implantation. Progesterone receptor (PGR), the cognate receptor of progesterone signaling, serves as the core regulator in coordinating the epithelial-stromal crosstalk in the endometrium compartment of the uterus. However, a detailed mechanism of how PGR works to modulate the uterine receptivity remains largely unclear. Our previous study revealed that the DNA motifs of PGR occupancy are enriched in the binding site of serum response factor (SRF), suggesting a potential association between PGR and SRF in modulating downstream factors for uterine functions. SRF is a transcription factor that regulates a versatile of biological functions, including cell proliferation, cytoskeletal remodeling, and cell motility. To investigate whether SRF plays a functional role in the female reproductive system, we ablated SRF in PGR-expressing tissues in mice and examined the phenotype. Results showed ablation of SRF leads to infertility in female mice due to both ovarian defects and impaired decidualization in the uterus, which implicates that SRF may regulate the hormonal responsiveness in the female reproductive tracts. To investigate the intrinsic effect of SRF loss on the uterus, we treated ovariectomized SRF knockout mice with either progesterone or estrogen, and subsequently performed RNA sequencing on mice uteri. Ingenuity pathway analysis performed on the 455 differential expressed genes (fold change>2, adjusted p-value<0.05) between SRF knockout and wildtype mice, showed that SRF is involved in the processes of inflammatory response, cell metabolism, cell cycle regulation, as well as fibrotic progression in mice uterus in a hormone-independent manner. More interestingly, from the comparisons among the groups treated with hormones, progesterone signaling is found to be suppressed whereas estrogen signaling was enhanced in the absence of SRF, indicating that SRF is critical to control the hormonal signaling in mouse uterus. Overall, these data indicated SRF loss could directly impact the uterine functions through affecting cell sensitization to hormones response. To further characterize whether SRF serves as a regulator of the signaling, our future direction will focus on the mechanistic study on the molecular network of how SRF and PGR interact to modulate the hormones response in the uterus.

Poster Presentation 35

Ternary crystal structure of neutralizing antibodies complexed with major peanut allergen Ara h 2

Min J, Pomés A, Patil S, Pedersen LC, and Mueller GA
Structure Function, DIR GISBL, NIEHS, Indoor Biotechnologies, Inc., Charlottesville, VA, USA, Food Allergy Center, Department of Pediatrics, Massachusetts General Hospital, Boston, Massachusetts, USA,

Peanut allergy is one of the most common causes of severe allergic reactions to food, affecting over 3 million people in the United States. Peanut Oral immunotherapy (OIT) is the most studied experimental therapy to develop sustained tolerance (ST) in peanut allergy patients. Among 17 identified peanut allergens, Ara h 2 is the most potent allergen. Successful OIT results in neutralizing antibodies against Ara h 2, which are reliable reagents for predicting the severity of the disease and the benefit of OIT. Based on a competitive analysis of anti-Ara h 2 antibodies cloned from patients undergoing peanut OIT, neutralizing antibodies (mainly IgGs) recognize both one linear and three conformational epitopes on Ara h 2. We determined the crystal structures of the S1, T1, and T5 neutralizing antibodies in ternary complexes with Ara h 2 at resolutions of 2.3 Å (S1/T1/Ara h 2) and 2.25 Å (T1/T5/Ara h 2), respectively. To the best of our knowledge, these are the first structures of human-derived antibodies in complex with an allergen. These complexes revealed the three different immunodominant conformational epitopes covering about 50 % of the Ara h 2 surfaces. We designed Ara h 2 double mutants to test the binding affinity to these neutralizing antibodies. We found that these double mutants show an affinity reduction of 3 order of magnitude compared to the wild type Ara h 2 with respect to their corresponding antibodies, suggesting the critical role of each residue on epitopes. These neutralizing antibodies may share conformational epitopes with anaphylaxis-causing IgE; Thus, the structure-based design of mutants will lead us to develop hypoallergenic variants of Ara h 2 with a reduced risk of adverse events during OIT.

Poster Presentation 36

GLIS3: A critical player in pancreatic ductal cell function

Pradhan T, Pradhan T, Kang H, Grimm S, and Jetten AM
Cell Biology, DIR IIDL, NIEHS, Integrative Bioinformatics Supportive Group,

GLIS3 is a Krüppel-like zinc finger transcription factor belonging to GLIS subfamily discovered in our lab. Altered GLIS3 expression and function plays an essential role in development and regulation of several endocrine functions. Loss of GLIS3 function causes neonatal diabetes, hypothyroidism, and polycystic kidney disease. Previously, our lab has reported specific localization of GLIS3 in ductal cell compartment in pancreas along with beta cells. However, the precise role of GLIS3 in pancreatic ductal cells is still unknown. The aim of our study is to identify the function of GLIS3 in pancreatic duct cells in relation to duct-associated diseases. To obtain insights into its function in these cells, we developed a human pancreatic duct cell line expressing doxycycline-inducible GLIS3 and performed RNA-Seq and ChIP-Seq analysis to identify genes that are directly regulated by GLIS3. RNA-seq analysis showed a significant enrichment of genes associated with aldosterone synthesis, insulin secretion, calcium signaling, cAMP signaling, and cell adhesion in GLIS3-expressing cells. Pancreatic ductal cells majorly secrete HCO3-(bicarbonate) to the pancreatic juice to aid digestion. cAMP and Ca2+ are two major modulators for HCO3- secretion by ductal cells and known to be altered in pancreatic diseases, including fibrosis and pancreatitis. Further, ChIP-Seq analysis identified many genes that are directly regulated by GLIS3, including *CAMK2A*, *CHRM3*, *ADCY4*/5 and *PLCE1*, which play a key role in the regulation of cAMP- and Ca2+-signaling. Taken together, these observations suggest a critical role for GLIS3 in the direct regulation of cAMP- and Ca2+-signaling pathways in human pancreatic ductal cells. We are further extending our study to understand the role of GLIS3 in the physiology of pancreatic duct using specific KO mouse models. We believe, our study would shed light on GLIS3 mediated molecular regulation in pancreatic ductal cell function and associated diseases.

Poster Presentation 37

Two Paths Diverged in the Fetal Mouse Ovary, Sorry I Could Not Travel Both

Rattan S, Liu C, Rodriguez K, and Yao HH
Reproductive Developmental Biology, , NIEHS, Reproductive Developmental Biology Group, Reproductive and Developmental Biology Group,

Ovarian dysfunction is a leading cause behind infertility in the USA. Dysfunction may result from defects in ovarian formation, particularly during fetal life. The formation of a functional ovary involves the orchestrated establishment of somatic cells. Somatic cell lineages are composed of supporting and interstitial cells, each necessary for various roles in normal ovarian functions. The development of the interstitial cells is complex due to diverse interstitial cell types found in adult ovaries. To define the developmental processes determining interstitial cell progression, we performed a time-course analysis of somatic cell fate progression in the mouse ovary from single-cell RNA sequenced data. We discovered a subpopulation of somatic cell progenitors expresses *Hes1*, a transcription factor indicative of NOTCH pathway activation. By utilizing genetic lineage-tracing techniques, we marked cells with *Hes1* expression during ovarian formation, and found that *Hes1*+ cells develop exclusively into interstitial cells in adult mouse ovary. This expression pattern led to the hypothesis that activation of NOTCH pathway defines interstitial cell fate whereas its absence marks supporting cells. To determine whether NOTCH signaling is necessary for interstitial cell establishment, NOTCH factors were removed from the somatic cell populations; however, development of interstitial cells still occurred. We next tested whether NOTCH pathway is sufficient to transform somatic cells by ectopically activating NOTCH pathway in somatic cells. Ectopic NOTCH activation resulted in defects of cell lineage specification with a reduction in steroidogenic interstitial, supporting, and ovarian stromal cells. These results illustrate that activation of NOTCH pathway was not sufficient to transform supporting cells into interstitial cells in the ovary; however, a properly tuned NOTCH pathway is necessary for normal somatic cell development in the ovary. These findings are necessary to identify factors responsible for establishing somatic cell lineages during ovarian development.

Poster Presentation 38

Food Insecurity and Sleep Health by Race/Ethnicity in the United States

Riley NM, Alhasan DM, Jackson II W, and Jackson CL
Social & Environmental Determinants of Health Equity Group, DIR EB, NIEHS, Social & Scientific Systems, Inc., a DLH Holdings Company, Durham, NC

Background: Food insecurity may influence sleep through poor mental health (e.g., depression) and immune system suppression. Although prior studies have found food insecurity to be associated with poor sleep, few studies have investigated the food security-sleep health association among racially/ethnically diverse participants and with multiple sleep dimensions.

Research Question/Hypothesis: Our research questions included, “Is food insecurity associated with poor sleep health in a nationally-representative sample of the United States (US)?” and “Does the association between food insecurity and poor sleep health vary by sex/gender and race/ethnicity?” We hypothesized that food insecurity would be associated with poorer sleep health and that the magnitude of associations between food insecurity and sleep health would be stronger among women than men and racial/ethnic minority groups than Non-Hispanic(NH)-White adults.

Research Design: Using National Health Interview Survey data, we examined overall, sex/gender-, and racial/ethnic-specific associations between food insecurity and sleep health. Food security was measured using ten questions based on the past 30 days that we categorized as very low, low, marginal, and high. Sleep duration was categorized as very short (<6 hours), short (<7 hours), recommended (7-9 hours), and long (≥9 hours). Sleep disturbances included trouble falling and staying asleep, insomnia symptoms, waking up feeling unrested, and using sleep medication (all ≥3 days/times in the previous week). Adjusting for sociodemographic characteristics and other confounders, we used Poisson regression with robust variance to estimate prevalence ratios (PRs) and 95% confidence intervals (95% CI) for sleep dimensions by very low, low, and marginal vs. high food security.

Results: Among 177,435 participants, mean age was 47.2±0.1 years, 52.0% were women, and 68.4% were NH-White. Among the 4.5% of individuals reporting very low food security, 56.6% were women and 53.4% were NH-White. After adjustment, very low vs. high food security was associated with a higher prevalence of very short (PR=2.61 [95%CI: 2.44-2.80]) and short (PR=1.66 [95% CI: 1.60-1.72]) sleep duration. Very low vs. high food security was associated with higher trouble falling asleep among men (PR=2.32 [95% CI: 2.16-2.49]) than women (PR=2.14 [95% CI: 2.04-2.25]). Very low vs. high food security was associated with higher prevalence of very short sleep duration among NH-Whites (PR=2.73 [95% CI: 2.50-2.99]) than NH-Blacks (PR=2.03 [95% CI: 1.80-2.31]).

Conclusion: Food insecurity was associated with poorer sleep in a racially/ethnically diverse sample of the US population and varied by sex/gender and race/ethnicity. Food insecurity may be intervened upon, with special consideration to sex/gender and race/ethnicity, to improve sleep.

Poster Presentation 39

Characterization of Treacle DNA Binding and Disease Mutations in Treacher Collins Syndrome

Salven DS, Parsons R, Tumbale P, and Williams R
Genome Integrity and Structural Biology Laboratory, DIR GISBL, NIEHS

Cellular DNA is constantly under assault from metabolic processes, radiation of various sorts, and exposure to environmental substances, resulting in DNA damage. Defects in DNA repair underlie human genetic diseases including neurodegeneration and cancer. Aprataxin (APTX) plays a crucial role in DNA repair by proofreading DNA ligation to prevent persistent DNA strand breaks, thereby maintaining genome integrity. Using targeted YFP-trap immunoaffinity proteomics coupled to mass spectrometry, we uncovered a novel APTX binding protein, the *TCOF1* gene product, Treacle, which may have a role in regulating APTX activity. Treacle is a nucleolar protein involved in ribosomal DNA gene transcription and pre-ribosomal RNA processing through its interactions with Upstream Binding Factor (UBF1) and RNA polymerase I (Pol I). In addition, Treacle functions as a transport protein recruiting the nuclear double-strand break repair factor NBS1 to the nucleolus in response to DNA damage. Results from our fluorescence microscopy experiments show that APTX and Treacle co-localize to the nucleolus. In addition, purified full-length or N-terminal fragments of Treacle stimulate APTX deadenylase activity. Interestingly, our electrophoretic mobility shift experiments (EMSA) demonstrate that Treacle itself possesses high-affinity DNA binding activity mediated through its central region acidic-basic amino acid rich repeats which may be important for Treacle's cellular functions associated with ribosome biogenesis and DNA repair. *TCOF1* has been implicated in Treacher Collins Syndrome (TCS), a severe autosomal dominant congenital disorder of craniofacial development. TCS mutations are found throughout the Treacle protein including the LIS1 homology (LisH) containing N-terminal domain. We determined a high-resolution X-ray structure of Treacle's N-terminal domain homodimer and performed structure-function characterization of seven TCS mutations mapped to Treacle's dimerization interface using biochemical and biophysical approaches. Our results show that Treacle dimerization is required for DNA binding. Treacle N-terminal TCS mutations adopt altered confirmations at the dimer interface, resulting in protein instability and defects in DNA binding. These findings provide new insights into TCS disease mechanism and reveal the novel DNA binding activity of Treacle which may be important for targeting protein partners including APTX to specific DNA structures.

Poster Presentation 40

PMCA1 regulates calcium signals at fertilization

Savy V, Shi M, Stein P, and Williams CJ
Reproductive Medicine, RDBL, DIR, and BCBB, DIR, NIEHS

Mammalian fertilization triggers a series of oscillations in the egg's intracellular Ca2+ level, which is the hallmark signal for egg activation. The oscillatory dynamic is also shaped by Ca2+ modulators present in the mature egg. Interestingly, the experimental modulation of Ca2+ levels following in vitro fertilization impacts embryo development and even offspring growth rate. In somatic cells, PMCAs play important roles in supporting calcium homeostasis, but a role for PMCA during fertilization remains unexplored. Here we tested the hypothesis that PMCA1 regulates Ca2+ homeostasis at fertilization. We found that in mouse eggs, the most highly expressed PMCA isoform is PMCA1. Because the PMCA1 null mouse is embryonic-lethal, we conditionally deleted PMCA1 (cKO) in oocytes using the Zp3-cre transgene. Females with cKO eggs are fertile. However, in vitro fertilized cKO eggs had abnormal calcium dynamics at fertilization. Total area under the curve of Ca2+ peaks indicated that cKO eggs have ~65% more Ca2+ signal than controls ($p<0.0001$). Also, cKO-eggs had larger Ca2+ stores than controls ($p <0.0004$). PMCA+/- (Het) offspring derived from WT females and HET males remain smaller than their PMCA+/+ siblings. Surprisingly, PMCA+/- (Het) offspring derived from females with cKO eggs and WT males (and increased Ca2+ at fertilization) are indistinguishable from WT pups derived from WT parents. These results suggest that abnormal calcium signaling in vivo impairs offspring growth rate. Our results show the importance of PMCA1 in maintaining Ca2+ homeostasis at fertilization and support the idea that abnormal calcium signaling at fertilization impacts offspring growth.

Poster Presentation 41

Cell-free DNA is predictive of cellular differentiation status in cardiac organoids

Silver BB, Gerrish K, and Tokar E
Molecular Genomics Core, DIR, Mechanistic Toxicology Branch, DNTP, NIEHS

Drugs and other chemicals can have many damaging off-target effects, such as cardiac injury. In addition, exposure to certain drugs or teratogens during development can cause fetal abnormalities, including heart defects. However, the cardiotoxicity of many compounds, particularly during developmental stages, remains unclear. Advances in efficient, non-invasive monitoring strategies are therefore needed to improve the safety, identification, and prediction of cardiotoxicants.

Liquid biopsies are valued for their potential as non-invasive diagnostic tools for early disease detection. One component of interest is cell-free DNA (cfDNA) which refers to free-floating DNA in the bloodstream or extracellular media, believed to be generated largely by apoptotic cells. Several parameters including concentration, fragment size, and sequence can be used to characterize cfDNA, and infer information about the cells from which it originated. However, to accurately deduce cellular health from cfDNA, we need a more thorough mechanistic understanding of how nucleic acids are released in response to events at the cellular level.

Here, we used a cardiac organoid model to identify key changes associated with cellular differentiation and cardiac development. We observed that the concentration of cfDNA fluctuates during cardiac organoid formation. Notably, increased cfDNA concentrations did not necessarily correlate with higher levels of apoptosis, suggesting that additional mechanisms of cfDNA release may be present during cardiac differentiation. Intriguingly, the fraction of mitochondrial cfDNA dropped sharply as the organoids differentiated, which could represent preferential retention of cells with higher mitochondrial counts as the organoids mature. In addition, we observed alterations in the prevalence of specific genomic regions in the cfDNA during differentiation, which could be reflective of transcription factor binding or epigenetic modifications. Our future efforts include the identification of additional cfDNA sequences that are impacted by differentiation and understanding how drugs and toxins impact the cfDNA profile of mature and developing cardiac tissues.

Poster Presentation 42

Loss of JAZF1 protects against High-Fat Diet-Induced gut microbial dysbiosis and Nonalcoholic Fatty Liver Disease

Srivastava C, Srivastava C, Grimm S, Randall T, DeGraff LM, Gruzdev A, and Jetten AM
Cell Biology, DIR IIDL, NIEHS, Integrative Bioinformatics Support Group, Knockout Mouse Core Facility,

JAZF1/TIP27 is a 27kD transcriptional co-regulator. GWAS studies have indicated that single nucleotide polymorphisms in the *JAZF1* gene are associated with increased risk of type 2 diabetes (T2D) and several autoimmune diseases. Diet induced obesity is a major risk factor for different metabolic disorders, including T2D and nonalcoholic fatty liver disease (NAFLD). Gut microbiota imbalance contributes to the pathogenesis of NAFLD/liver steatosis, yet the underlying mechanism linking JAZF1 with gut microbiota in NAFLD progression remains obscure. To obtain greater insights into the physiological functions of JAZF1, we generated *Jazf1* null mice (*Jazf1-/-*) and fed them a high fat diet (HFD) for 8 to 15 weeks. HFD resulted in a significantly increased hepatic steatosis and obesity phenotype, in WT mice, that was found to be suppressed in HFD- *Jazf1-/-* mice. The gut microbiota was analyzed by 16s rRNA gene sequencing and phylogenetic reconstruction of unobserved states analysis was characterized in WT and *Jazf1-/-* mice fed with HFD for different time points (week 0 (control), week 4 and week 8). HFD fed WT mice showed an increase in NAFLD promoting bacteria (*Lactococcus, Lachnospiraceae and Bacteroides*). Interestingly, lack of JAZF1 protected HFD induced-gut microbial dysbiosis. MiSeq-results showed a decrease in NAFLD promoting bacteria (*Lactococcus, Lachnospiraceae and Bacteroides*) along with an increase in bacteria genera (*Muribaculaceae* and Oscillospiraceae) that prevent diet induced-gut microbial dysbiosis. These NAFLD promoting bacteria influence inflammation by releasing peptidoglycans and lipopolysaccharide, bacterial DNA etc., that targets CD14 and downstream toll-like receptor signaling in liver and in other tissues. These observations are consistent with our RNA-seq and qPCR data showing a significant downregulation in toll-like receptor signaling pathway and inflammatory response genes in HFD- *Jazf1-/-* mice liver. Taken together, our results suggests that loss of JAZF1 maintains the normal gut microbial balance and suppressing inflammatory signaling genes, thereby protecting mice from developing diet induced-NAFLD.

Poster Presentation 43

Urinary phthalate metabolite mixtures in pregnancy in relation to fetal growth

Stevens DR, Keil AP, Bommarito P, McElrath T, Trasande L, Barrett ES, Bush NR, Nguyen R, Sathyanarayana S, Swan S, and Ferguson KK
Perinatal and Early Life Epidemiology, DIR EB, NIEHS, Epidemiology Branch, National Institute of Environmental Health Sciences, Durham, NC, USA, and Department of Epidemiology, The University of North

Background: Prenatal phthalate exposure has been linked to reductions in fetal growth in animal and laboratory studies, but epidemiologic evidence is equivocal.

Objectives: 1) Examine the associations of prenatal phthalate metabolite mixtures with fetal growth, and 2) Examine effect modification by infant sex and omega-3 intake in pregnancy.

Methods: Analyses included 604 singleton pregnancies from TIDES, a prospective pregnancy cohort with spot urine samples and questionnaires collected in each trimester. The geometric means of specific-gravity corrected phthalate metabolites were calculated and log-transformed. Fetal growth outcomes included birthweight and length, and ultrasound measures of estimated fetal weight, abdominal circumference, head circumference, and femur length at 14 and 27 gestational weeks. We used a novel application of quantile g-computation to estimate a joint association between the phthalate metabolites and fetal growth outcomes, and to determine effect modification by infant sex or omega-3 intake.

Results: A one-quartile increase in pregnancy-averaged phthalates was associated with reduced birthweight (β (95% confidence interval): -50.72 (-111.48, 10,04), p=0.10) grams and length (-0.18 (-0.54, 0.18), p=0.33) centimeters. There were no notable differences in ultrasound measures of fetal growth by exposure, but some differences in effects by infant sex and omega-3 intake. The association between the phthalate metabolite mixtures and reduced fetal growth was strongest among participants with adequate omega-3 intake, and female fetuses experienced reduced weight whereas male neonates experienced reduced length with increasing exposure.

Conclusion: Prenatal phthalate exposure may contribute to reduced size at birth, and reduced fetal growth in certain subgroups.

Poster Presentation 44

Preconception Vitamin D and Miscarriage in a Prospective Time to Pregnancy Study

Subramanian A, Steiner AZ, Weinberg CR, and Jukic AZ
Fertility and Reproductive Health, DIR EB, NIEHS, Department of Obstetrics and Gynecology, Duke University, Biostatistics and Computational Biology Branch, NIEHS,

Background: In humans, low vitamin D has been associated with prolonged menstrual cycles, delayed ovulation, and lower conception rates. Animal and in vitro data indicate that vitamin D may affect implantation. Our objective was to estimate the association between preconception vitamin D level and risk of miscarriage.

Methods: Participants were from Time to Conceive, a prospective time-to-pregnancy cohort in North Carolina. Participants were trying to conceive naturally for 3 months or less at enrollment and were aged 30-44 years. A blood sample was collected during the preconception period and 25-hydroxyvitamin D [25(OH)D] was measured. Women who conceived (n=362) were at risk of miscarriage from the day of a reported positive pregnancy test until pregnancy end which was either a participant-reported pregnancy loss or 20 weeks (for pregnancies that lasted longer than 20 weeks). Gestational age at the end of the pregnancy was defined by ovulation. Time to miscarriage (days) or censoring was modeled using a multivariate Cox proportional hazards model. Multiple imputation was performed to impute missing covariates and the day of ovulation.

Results: Mean (SD) age was 33 (3.0) years. As expected, mean 25(OH)D was lower among those who reported their race as African American and, those with higher BMI. Unadjusted 25(OH)D was not associated with miscarriage. After adjustment for age, race, BMI, education, exercise, alcohol, and caffeine intake, compared to the referent group (30-40 ng/ml), the hazard ratio (HR) and 95% confidence interval (CI) for those with a 25OHD level of less than 30 ng/ml was 1.10 (CI: 0.63, 1.93). Among participants with a 25OHD level of at least 40 ng/ml the HR was 1.04 (CI: 0.61, 1.79).

Conclusion: Vitamin D was not associated with risk of miscarriage in this analysis, but has been in previous studies. Additional studies are necessary to resolve the conflicting literature and to determine if vitamin D is efficacious in preventing miscarriage.

Poster Presentation 45

High-Resolution X-Ray Structures of DNA ligase 1 Reveal the Molecular Mechanisms of High-Fidelity DNA Ligation and LIG1 Syndrome

Tumbale PP, Jurkiw T, Schellenberg MJ, Riccio A, Cunningham-Rundles C, O'Brien P, and Williams R
Genome Stability Structural Biology, DIR GISBL, NIEHS, Department of Biological Chemistry, University of Michigan, Ann Arbor, MI, USA, Division of Clinical Immunology, Departments of Medicine and Pedi

DNA ligases catalyze the joining of DNA nicks to finalize DNA replication, recombination, and repair transactions. Human DNA ligase 1 (LIG1) is recognized to be the primary replicative ligase and associates with the replisome to finalize Okazaki fragment maturation, completing more than 50 million ligation events during each cycle of DNA replication. To protect integrity of the genome, LIG1 efficiently seals DNA breaks bearing correct Watson-Crick base pairs but aborts ligation before nick sealing to prevent phosphodiester bond formation at DNA junctions harboring mutagenic lesions such as mismatches, oxidative damage, base insertion and deletion, and incorrect sugar. How such high-fidelity (HiFi) ligation is enforced is unknown. We report high-resolution X-ray structures of LIG1-DNA complexes showing that LIG1 employs Mg2+-reinforced DNA binding to validate DNA base pairing of the ligated 3' terminus. Analysis of LIG1 reaction kinetics and X-ray structural results show that this HiFi-Mg2+ site normally impedes LIG1 catalysis on oxidatively damaged substrates. Conversely, HiFi-Mg2+ site mutants exhibit suppressed ligation fidelity, and readily perform mutagenic ligations with 8-oxoG paired termini. Our results support a model where ligation fidelity is reinforced by the LIG1 enzyme which is tuned to release mutagenic substrates. In a second shell of protection, the intrinsic fidelity of LIG1 is surveilled by Aprataxin (APTX)-regulated suppression of mutagenic and abortive DNA ligation at oxidative DNA damage.

LIG1 has been implicated in immunological disorder. Immune compromised patients harbor hypomorphic *LIG1*alleles encoding substitutions of conserved arginine residues, R771W and R641L, that compromise LIG1 activity through poorly defined mechanisms. To understand the molecular basis of LIG1 syndrome mutations, we determined high resolution X-ray structures and performed systematic biochemical characterization using steady-state and pre-steady state kinetic approaches. Our results unveil a cooperative network of plastic DNA-protein interactions that connect DNA substrate engagement with productive binding of Mg2+ cofactors for catalysis. LIG1 syndrome mutations destabilize this network, compromising Mg2+ binding affinity, decreasing ligation efficiency, and leading to elevated abortive ligation that may underlie the disease pathology. These findings provide novel insights into the fundamental mechanism by which DNA ligases engage with a nicked DNA substrate.

Poster Presentation 46

Toenail and serum measures as biomarkers of iron levels

Von Holle AF, O'Brien KM, Sandler DP, Janicek R, Karagas MR, White AJ, Jackson BP, and Weinberg CR
Methods and Applications in Epidemiology, DIR BCBB, NIEHS, DIR EPID, NIEHS, University of Minnesota, Dartmouth University,

Background: For epidemiologic studies, iron measurements are often based on serum. Toenails offer a convenient alternative to serum because of ease of collection, transport, and storage. Very few contemporary studies have examined the correlation between the serum and toenail measures for trace metals, including iron. If similar, toenail samples could provide a valid substitute for serum biomarkers. Our aim was to compare measures using serum and toenail samples both on a cross-sectional and longitudinal basis from a subcohort of women in the United States.

Methods: Using a sample from the US-wide prospective Sister Study cohort, we compared trace iron levels in toenails with three serum biomarkers: iron, ferritin and percent transferrin saturation. A sample of participants (n=146) donated both blood and toenails at baseline (2003-2009) and a subsample (59%, n=86) provided specimens again about 8 (interquartile range: 7,9) years later. Cross-sectional analyses included Spearman's rank correlation to assess toenail/serum association and coefficients of variation. We also considered maintenance of rank across time separately for toenails and for serum and compared Spearman's correlation coefficients of repeated measures for toenail and serum values. Longitudinal analyses also included mixed-effects models to estimate and compare change in iron levels over time.

Results: Overall, toenail and serum iron values did not correlate well with each other. Spearman correlations with toenail measures at baseline (follow-up) were 0.08 (0.09) for serum iron, 0.08 (0.07) for transferrin saturation, and -0.09 (-0.17) for ferritin. The Spearman correlation for toenail iron between repeats across the two time points (0.47, 95% CI: 0.30, 0.64) was higher than for serum iron (0.30, 95% CI: 0.09, 0.51), transferrin saturation (0.34, 95% CI: 0.15, 0.54), and lower than that for ferritin (0.58, 95% CI: 0.43, 0.73). When assessing changes over time by menopause status, there was a 7.1% (95% CI: 3.7, 10.5) relative increase in serum ferritin per year increase in age for women who transitioned from pre- to postmenopause status during the follow-up period. In contrast, toenail iron decreased 3.5% (95% CI: -6.1, -0.8) per year for this group.

Summary: Based on cross-sectional and longitudinal analyses, iron measures based on serum did not correlate with those based on toenails. Toenail iron measures appear to be moderately repeatable, but cannot be taken as a proxy for serum iron values and may represent different mechanisms or compartments of iron storage.

Poster Presentation 47

Exploration of Cell-Free DNA as a Potential Biomarker of Teratogenicity Using a Human Embryonic Stem Cell Culture Model

Weick MI, Chen I, Silver B, Gladwell W, Wu X, Tokar E, Foley JF, Merrick BA, and Gerrish K
Mechanistic Toxicology Branch, DNTP, NIEHS, Mechanistic Toxicology Branch, DNTP, NIEHSMechanistic Toxicology Branch, DNTP, NIEHS, Molecular Genomics Core, DIR, NIEHS,

Embryoid bodies derived from human embryonic stem cells (hESCs) are helpful as high throughput assay for testing teratogens due to their ability to differentiate spontaneously into the three germ layers. Cell-free nucleic acids are liquid biopsy molecules being investigated as emerging noninvasive biomarkers for various diseases' early detection, prognosis, prediction, and pharmacodynamic responsiveness. Liquid biopsy samples are problematic for cell-free DNA (cfDNA) analysis since numerous sources and causes of DNA are released into circulation. *In-vitro* models offer the advantage of a closed system, free of contamination by multicellular sources. We explored conditioned media from hESCs for the potential of using cfDNA as a biomarker of teratogenicity. To accomplish this, the conditioned media were collected from the H9 hESCs that had been exposed to known and potential teratogens. CfDNA was extracted, and fragment analysis was completed. There did not appear to be any differences in cfDNA concentration or fragmentation profiles in response to the chemicals tested. Droplet Digital PCR (ddPCR) partitions nucleic acid samples into thousands of nanoliter-sized droplets. PCR amplification is carried out within each droplet, enabling the absolute quantitation of nucleic acids in a sample. Our preliminary analyses have demonstrated that ddPCR is an effective assay to measure the presence of specific targets present in cfDNA samples extracted from conditioned media, indicating its ability to be used as a tool to identify the respective germ cell layers. To determine if individual germ layers are affected by the exposures, we have designed ddPCR assays to assess the presence of germ layer markers in the cfDNA collected at three time points (Days 2, 6, and 10) during the chemical exposure. We propose that these assays may allow us to evaluate germ layer variation following exposure to teratogens.

Poster Presentation 48

Functional characterization of the SARS-CoV-2 Nsp15 endoribonuclease N-terminal domain and beyond.

Wilson IM, Frazier MN, Li J, Randall T, and Stanley RE
Nucleolar Integrity, DIR STL, NIEHS, Integrative Bioinformatics Support Group,

The coronavirus pandemic has ignited research worldwide to better understand how to respond to emerging health threats. COVID-19 is the disease caused by SARS-CoV-2, a novel coronavirus that emerged in 2019 from a family of viruses that the world of research and medicine has seen before. Its close cousins SARS-CoV and MERS plagued the world in 2002 and 2012, respectively. While the data presenting the statistics of vaccination campaigns worldwide is promising, the emergence of SARS-CoV-2 variants due to the lack of vaccine availability and the rise of anti-vaccination movements highlight the need for anti-viral therapeutics. One such therapeutic target is the viral protein Nsp15, an endoribonuclease that is conserved across all coronaviruses. Nsp15 helps regulate the amount of SARS-CoV-2 RNA within infected cells by cleaving viral RNA 3’ of uridines, such as within the poly U stretch at the 5’ end of the negative strand of SARS-CoV-2. This allows the virus to evade triggering an immune response and helps hide the virus from host dsRNA pattern recognition receptors, such as MDA5. With knowledge of new viral variants emerging, it is important to study how Nsp15 has evolved over the pandemic. In combination with previous structural data, bioinformatics analyses of 1.9+ million SARS-CoV-2 sequences revealed several mutations across Nsp15's three structured domains. These Nsp15 variants were characterized biochemically and their enzymatic activity was compared to wild type Nsp15. We found that mutations to important catalytic residues decreased cleavage activity, while variants with higher prevalence largely showed either increased activity or no change. Overall, our work is helping to establish how Nsp15 has evolved during the course of the pandemic.

Poster Presentation 49

Socioeconomic Position During Childhood and Over the Life Course and its Association with Obesity in Adulthood

Woo JM, Bookwalter DB, and Sandler DP
Chronic Disease Epidemiology, DIR EB, NIEHS, Westat

Importance: The association between childhood socioeconomic position (SEP) and adult obesity risk, independent of adult SEP, has yet to be fully elucidated.

Objective: To determine the effect of childhood SEP and SEP trajectory on adult obesity.

Design: We use baseline data from the Sister Study, a prospective cohort of US women aged 35 to 74 years (N=50,884; enrollment between 2003-2009).

Setting: The Sister Study includes participants from all 50 states and Puerto Rico.

Participants: Eligible participants had available baseline anthropometric data and at least one measure of childhood SEP (N=50,849).

Exposures: Measures of SEP were collected via self-administered questionnaire at baseline. Confirmatory factor analysis was used to create continuous latent variables for childhood and adult SEP. Latent class analysis was used to identify 5 latent SEP trajectories, representing changes between childhood and adult SEP.

Main Outcomes and Measures: Height and weight were measured at baseline and used to assess obesity (body mass index >30 kg/m2). We used log-binomial regression models to estimate relative risk (RR) and 95% confidence intervals (95%CI) of childhood SEP and SEP trajectories on adult obesity. Mediation models were used to assess the natural direct effect of childhood SEP on adult obesity and the natural indirect effect via adult SEP.

Results: Approximately 30% of participants were classified as obese at baseline. Lower childhood SEP was associated with a greater risk of obesity at baseline (RR=1.16, 95%CI: 1.14-1.18), after adjusting for covariates. In race/ethnicity stratified models, estimates were still elevated, but largely attenuated, for Black and non-Black Hispanic/Latina participants. The direct effect of childhood SEP persisted in mediation models independent of adult SEP (RR=1.11, 95%CI: 1.08-1.14). Adult obesity risk was elevated for all SEP trajectories compared to the SEP trajectory characterized by persistent high socioeconomic advantage.

Conclusions and Relevance: Our findings suggest that childhood SEP may be an important risk factor of adult obesity independent of SEP later in life, with mediating pathways that may differ by race/ethnicity. These results support the importance of culturally sensitive and timely interventions, particularly during childhood, in obesity prevention.

Poster Presentation 51

Liver cancer cells that survive methionine restriction develop phenotypes of persistent cancer cells

Xu Q, and Li X
Metabolism, Genes, and Environment, DIR STL, NIEHS,

Liver cancer, the third leading cause of global cancer death, is notoriously resistant to conventional chemotherapy or radiotherapy. Our previous study indicates that liver cancer cells expressing high levels of hepatocyte nuclear factor 4a (HNF4a) are sensitive to methionine restriction (MR), a dietary intervention that inhibits tumor growth and improves cancer therapy. However, we observed some cells managed to evade MR-induced cell death. These cells developed typical phenotypes of persistent cancer cells with slow proliferation and altered cell identity. Cells that survived MR acquired capability of migration and displayed upregulation of markers for epithelial-to mesenchymal transition (EMT), a process that is often associated with tumor metastasis and drug resistance. In addition, depletion of methionine, the only sulfur-containing essential amino acid, significantly changed the expression of key enzymes involved in metabolism of sulfur amino acids (SAA). We intend to further investigate how rewired SAA metabolism may promote the survival of liver cancer cells under MR.

Poster Presentation 52

Cadmium exposure alters migration dynamics and increases heterogeneity of human uterine fibroid cells - insights from time-lapse analysis

Yan Y, Shi M, Fannin R, Yu L, Liu J, Castro L, and Dixon D
MTB, DNTP, NIEHS, Biostatistics & Computational Biology Branch, NIEHS, Molecular Genomics Core Laboratory, NIEHS,

Cadmium (Cd) is one of the most prevalent environmental heavy metal contaminants and is considered an endocrine disruptor and carcinogen. In women with uterine fibroids, there is a correlation between blood Cd levels and fibroid tumor size. In this study, fibroid cells were exposed to 10 μM CdCl2 for 6 months and a fast-growing Cd-Resistant Leiomyoma culture, termed CR-LM6, was recovered. To characterize the morphological and mechanodynamic features of uterine fibroid cells associated with prolonged Cd exposure, we conducted time-lapse imaging using a Zeiss confocal microscope with 3x3 tile scanning. The resulting time-series files were stitched by Zen Black and analyzed by Imaris and R statistical package. Our experiments recorded more than 64,000 trackable nuclear surface objects with each having multiple parameters such as nuclear size and shape, speed, location, orientation, track length, and track straightness. Quantitative analysis revealed that prolonged Cd exposure significantly altered cell migration behavior, such as increased track length and reduced track straightness. The Cd exposure also significantly increased heterogeneity in size and shape of nuclei. Additionally, Cd exposure significantly increased the median and variance of instantaneous speed, indicating that Cd exposure results in higher speed and greater variation in motility. The mRNA profiling by NanoString and IPA strongly suggested that the direction of gene expression changes due to Cd exposure enhanced cell movement and invasion. The altered expression of ECM proteins such as collagens, which are required for migration contact guidance, may be responsible for the greater heterogeneities in morphodynamics. The significantly increased heterogeneity of nuclear size, speed, and altered migration patterns may be a prerequisite for fibroid cells to attain characteristics favorable for cancer progression, invasion, and metastasis.

Poster Presentation 53

Impact of Vitamin D Deficiency on Defective In Vivo and In Vitro Decidualization

Yi M, Jukic AZ, and DeMayo FJ
Pregnancy & Female Reproduction, DIR RDBL, NIEHS, Fertility and Reproductive Health, DIR EB, NIEHS, Pregnancy & Female Reproduction, DIR RDBL, NIEHS

Existing evidence has suggested that unfavorable pregnancy outcomes are highly related to dietary supplement and environmental factors. One key nutrient important for human health is Vitamin D, VitD (1-3). Many epidemiological studies have demonstrated that VitD deficiency in humans may impact female reproductive ability, and one way to alleviate adverse environmental exposures is taking VitD (2, 4-7). VitD acts, in part, *via* its receptor the Vitamin D receptor, VDR, a ligand dependent transcription factor. Ablation of the VDR in the whole mouse impacts female reproduction (8). Given its emerging role in fertility the goal of this study was to investigate the role of Vitamin D in female reproduction *in vivo* using a Vitamin D deficient, VitD Def, mouse model and *in vitro* using a human endometrial stroma cell line, T-HESC.

Vitamin D deficiency in mice was achieved by feeding 6 weeks of age, female C57Bl/6J mice either vitamin D3 adjusted (1000 IU/kg) or deficient diets for 9 weeks in total. The impact of Vit D Def was then assessed by assaying the ability of the mouse uterus to undergo a hormonal induced decidual response. Mice were ovariectomized (OVX) after 5 weeks on either diet. Mice were then given the standard regimen of ovarian steroids to induce decidualization. A decidual stimulus of sesame oil was then injected into one uterine horn and after 5 days the weight ratio of the stimulated horn to the control horn. The weight ratio of the oil-injected over the un-injected uterine horn indicated that the robust decidualization occurred in all the adjusted diet-fed mice, but in the deficient diet-fed mice, showed an impaired decidual response with decreased weight ratio of the stimulated uterine horn to the control horn.

In vitro studies were performed with immortalized human endometrium stromal cells (T-HESC). T-HESCs were decidualized in culture with E2, medroxyprogesterone acetate, and dibutyryl cAMP for 72 hr in the presence or absence of 1,25(OH)2D3, and in the presence of siRNA of vitamin D receptor (*VDR*) or non-targeting. The ability of the T-HESC to decidualized was determined by measuring the expression of prolactin (*PRL*) and insulin-like growth factor-binding protein-1 (*IGFBP-1*). Surprisingly, the decidual marker genes were significantly increased in the *VDR* knockdown cells, and in the presence of 1,25(OH)2D3. This would indicate that for appropriate stroma cell function *VDR* may repress stroma cell differentiation and this repression is alleviated by administration of the ligand.

In summary, Vitamin D is critical for normal uterine function in the mouse *in vivo* and human endometrial stroma cells *in vitro.* We are currently determining the impact of VitD Def on other reproductive parameters in mice and the impact of reproductive tract ablation of VDR on female reproduction. Also, we are now investigating the cistrome and transcriptome of VitD in T-HESC. This work will define the role of Vitamin D on female reproductive health.

Poster Presentation 54

INO80 Remodels Bivalent Chromatin in Pluripotent State Transition

Yu H, Wang J, Lackford B, Bennett B, Li J, and Hu G
Stem Cell Biology, DIR ESCBL, NIEHS, Integrative Bioinformatics Support Group, NIEHS

The INO80 chromatin remodeler is involved in many chromatin-dependent cellular functions. However, its role in pluripotency and cell fate transition is not fully defined. We examined the impact of *Ino80* deletion in the naïve and primed pluripotent stem cells. We found that *Ino80* deletion had minimal effect on self-renewal and gene expression in the naïve state, but led to cellular differentiation and de-repression of developmental genes in the transition toward and maintenance of the primed state. In the naïve state, INO80 pre-marked gene promoters that would adopt bivalent histone modifications by H3K4me3 and H3K27me3 upon transition into the primed state. In the primed state, in contrast to its known role in H2A.Z exchange, INO80 promoted H2A.Z occupancy at these bivalent promoters and facilitated H3K27me3 installation and maintenance as well downstream gene repression. Together, our results identified an unexpected function of INO80 in H2A.Z deposition and gene regulation. We showed that INO80-dependent H2A.Z occupancy is a critical a licensing step for the bivalent domains, and thereby uncovered an epigenetic mechanism by which chromatin remodeling, histone variant and modification coordinately control cell fate.

Poster Presentation 55

Role of TUT4 and TUT7 in spermatogonia differentiation

Morgan M, Kumar L, Li Y, Baptissart M, and Gupta A
Cell Differentiation, DIR RDBL, NIEHS,

Spermatogonia proliferation and differentiation are critical for the continuity of the spermatogenic linage and the production of functional sperm. Upon exposure to Retinoic Acid (RA), the undifferentiated spermatogonia show irreversible changes in morphology to become differentiating spermatogonia with no self-renewal capacity. The spermatogenic transcriptional program is controlled at many levels, including post-transcriptional regulation mediated by RNA modifications. One of the most critical mRNA modifications is the addition of a poly(A) tail at the transcript 3' end, which regulates the transcript's metabolism. Here, we focus on the Terminal Uridyl-Transferases TUT4 and TUT7 (TUT4/7), two enzymes known to promote mRNA degradation by poly(A) tail uridylation, in order to understand how post-transcriptional modifications to the mRNA 3' end regulate spermatogonia differentiation. We observed that TUT4/7 are restricted to spermatogonia, and other germ cells, in the testis. We found that depletion of TUT4 globally in mice significantly reduced the proliferation of germ cells and sperm count; however, mice are fertile. On the contrary, TUT7-depletion in the testis results in a decline in sperm count and fertility rate without affecting the proliferation of germ cells. To define how TUT4-mediated uridylation shapes the spermatogonia transcriptome, we established the 2S (synchronization and sorting) method for the isolation of undifferentiated and differentiated spermatogonia. We then performed poly(A) profiling together with quantification of terminal uridylation for undifferentiated and differentiated wild-type spermatogonia. We observed TUT4 characteristic uridylation of short poly(A) tails in both spermatogonial compartments, indicating a role for the proteins in the clearance of transcripts as cells transit towards more differentiated stages. Current experiments aimed to define the poly(A) profile in TUTs-deficient spermatogonia will identify critical targets required for spermatogonia differentiation. Understanding the molecular mechanism responsible for testis size reduction will help elucidate some of the causes leading to reduced sperm count currently observed in various human populations.

National Institute of Environmental Health Sciences
National Institutes of Health • U.S. Department of Health and Human Services